A Comparison of EMT, Dynamic Phasor, and Traditional Transient Stability Models

by

Rae Rui Ooi Yang

A Thesis Submitted to the Faculty of Graduate Studies of

The University of Manitoba

In partial fulfillment of the requirements of the degree of

Master of Science

Department of Electrical Engineering

Faculty of Engineering

University of Manitoba

Winnipeg, Manitoba Canada

ABSTRACT

This thesis presents a transient stability method using dynamic phasors. This method can be used to investigate low frequency (<5Hz) and sub-synchronous frequency (5Hz-60Hz) oscillations. It has major advantages as compared to traditional transient stability method and EMT method. It allows modeling of higher-frequency oscillation possible using time domain simulations, which is not achievable with conventional method. It also can be simulated at much larger time step as compared to PSCAD/EMTDC simulation. Comparison of the results with traditional model and detailed EMT model are also present, and they show very accurate results at frequency ranges up to 60Hz.

Keywords: Transient stability analysis, Dynamic Phasors, Single Machine Infinite Bus (SMIB), 3-phase fault, generator model, sub-synchronous resonance, IEEE first Benchmark model for sub-synchronous analysis,

ACKNOWLEDGEMENTS

First, I would like to thank my parents for believed that I can always do better than I believed in myself. They had always encouraged me to reach for the stars and supported me the best way they knew.

Secondly, my sincere gratitude must go to Dr. Udaya Annakkage, Dr. Chandana Karawita, and Dr. David Jacobson for their continuous advice, guidance and encouragement throughout this research work and beyond. It is a privilege and I am grateful that I have known and worked under their guidance.

Next, I would like to thank my husband for his understanding and support during my difficult times, and my daughters for not disrupt mommy when I am working on my research. I would also like to thank my friends and colleagues for their encouragement and support.

Lastly, not least, I would like to thank Manitoba Hydro for providing financial support for my continuing education.

DECLARATION

I certify that research work titled "*Transient Stability Simulation using Dynamic Phasors*" is my own work. The work has not been presented elsewhere for assessment. Where material has been used from other sources it has been properly acknowledged / referred.

Signature of Student

Rae Yang

6602653

Table of Contents

LIST OF FIGURES

CHAPTER 1 INTRODUCTION

1.1 Background

Due to re-structuring of the electricity market, aging of the power system infrastructures, use of new technologies and controls, operating in highly stressed conditions, stability of the power system becomes increasingly important. Currently, voltage stability, frequency stability, transient stability, inter-area oscillations are of great concern. As the interconnected power system becomes more complicated, more accurate system modeling is required to analyze various stability issues. More frequent blackouts recently have illustrated the importance of more accurate tools [11].

Power system stability consists of three main areas: frequency stability, voltage stability, and rotor angle stability [2]. Both frequency and voltage stabilities can be short term and long term, and may vary from few seconds to tens of minutes. Frequency stability is the ability of the power system to maintain steady frequency after subjected to a disturbance that causes imbalance between the generation and load. Instability may result in the form of sustained frequency swings that could trip off generations and/or loads. Voltage stability is the ability of power system to maintain steady voltage at all buses after subject to either a small or large disturbance that cause imbalance between load demand and load supply. The instability could result in tripping of transmission lines, loss of load in an area, and tripping of other elements by protection systems. The consequences of voltage instability could be severe; it could lead to cascading outages that result in voltage collapse. Rotor angle is a short term phenomenon, and can be sub-

divided into small-disturbance angle instability and transient stability. This thesis mainly investigates the transient stability subcategory in the rotor angle stability category. It will be explained in detail in this chapter and in relevant subsequent chapters. The classification of various power system stability phenomena and their subcategories are shown in figure 1 [2].

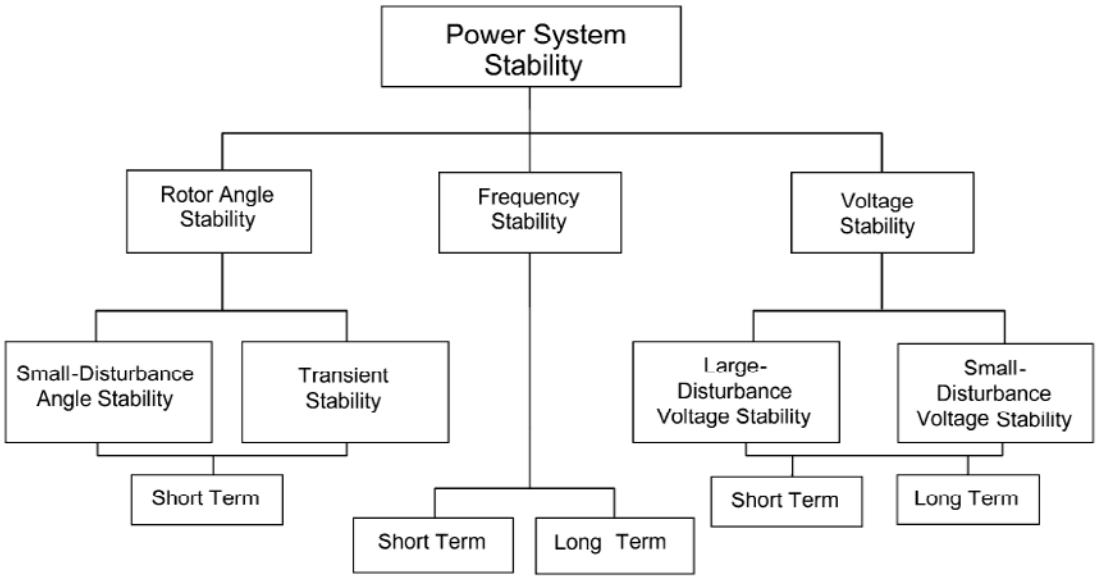

Figure 1 Classification of Power System Stability [2]

Rotor angle stability is the ability of the power system to restore equilibrium after a large system disturbance. It involves the study of the electromechanical oscillations inherent in a power system. The input mechanical torque and the output electromagnetic torque of each generator are in equilibrium under steady-state conditions. Disturbance in the system results in either accelerating or decelerating of the rotors. This could lead to increased angle separation. Since the power-angle relationship is non-linear, an increase in angle separation is accompanied by a decrease in power transfer beyond certain limits. Instability results if the kinetic energy corresponding to rotor speed differences cannot be

absorbed by the system after the fault is removed. It is usually evident within 3 to 5 seconds after the initial disturbance [2] [6]. Transient stability highly depends on the initial operating state of the system and the severity of the disturbance. It is categorized as a short term phenomena.

Currently, the most common techniques used for stability assessments are Electro-Magnetic Transient Type (EMTP) time domain simulation, transient stability (large signal disturbance), and small signal stability assessment. Only large signal disturbance will be considered for this thesis, therefore, the EMTP time domain simulation and transient stability will be analyzed.

EMTP type simulation uses detailed models, and it gives more accurate results than the transient stability analysis technique. In terms of this thesis, frequencies in the range up to 60Hz can be observed and analyzed accurately. The major drawback of EMTP simulation is the computation speed due to small time step, which results in slow simulation time. For this reason, only small power systems can be modeled and the oscillations in a large system cannot be observed accurately.

The traditional transient stability analysis technique uses simplified generator models which neglect stator transients, and the AC network is represented by constant admittance/impedance models, therefore it is computationally efficient and large power system can be modeled and analyzed. The disadvantage of this modeling technique is that the machine stator transients and AC network transients are neglected, only slow transients up to 5Hz can be captured, and fast transients in the range up to 60Hz cannot be observed.

In order to overcome the disadvantages of EMT type simulations and traditional transient stability analysis, Dynamic Phasor (DP) model will be implemented. Several advantages have been reported with using the time-varying fundamental frequency dynamic Phasor to model transient stability analysis. Firstly, it eliminates the need to model a complete representation of a large power system in a full time domain simulation, which is difficult and not useful in some cases. Secondly, DP can compute fast electromagnetic transients with larger time steps, thus, reduces simulation time as compared to EMT type simulations, and reduces the burden associated with representing network voltages and currents in time-domain [24][25]. The DP approach is viewed as the intermediate between the detailed time domain simulation (EMT) and the quasi-static sinusoidal steady-state approximation [26]. In this research, DP will be used to model and observe high frequency oscillations up to 60Hz for a large power system. The model includes the AC network dynamics by modeling the transmission system using Dynamic Phasors, and generator stator dynamics by including stator flux terms. The integration time steps used for the proposed model will also prove to be significantly larger than the detailed PSCAD/EMTDC platforms. The results will be compared to EMT and traditional transient stability analysis methods.

The comparison of the Constant Admittance type, Dynamic Phasor type and EMT Type models in terms of speed, accuracy, system size, frequency range, and model requirements are presented in Table 1.

Table 1 Comparison Summary of Constant Admittance Model, Dynamic Phasor Model and EMT Model

	Constant Admittance Type	Dynamic Phasor Type	EMT Type
Speed	Fastest	Faster	Slowest
Accuracy	Acceptable	Accurate	Very Accurate
System Size	Large	Medium	Small
Frequency Range	Less than 3Hz	Up to 60Hz	Up to few kHz
Model Requirement	Simplified	More Detailed	Very Detailed

1.2 Thesis Objectives

The main objective of this thesis is to analyze transient stability phenomena using dynamic Phasors (DP). This approach uses different modeling technique to represent synchronous machine and AC network components than from the traditional methodology. The following objectives will be achieved for this project.

A simple single-machine-infinite-bus (SMIB) system will be modeled to include stator fluxes in the synchronous generator; AC network components will be modeled using dynamic Phasors to represent all the transformers, transmission lines, static loads. This model will be compared to the traditional approach of using network matrix to represent the AC network, and generators modeled without the effects of stator fluxes and stator voltages is assumed to be constant. This model will also be benchmarked with detailed EMT model simulated in PSCAD/EMTDC software.

This SMIB system will be extended to model the IEEE first benchmark model to analyze sub-synchronous resonance phenomena to further verify the purposed methodology. The generator and the AC network components will be modeled using the same technique as the SMIB. The rotor will be modeled using a multi-mass turbine system instead of a single mass element. The sub-synchronous phenomena will be analyzed with various levels of transmission line compensation. The results will be compared with detailed EMT simulations.

One additional objective is to verify that the DP model can be simulated using larger time steps than the conventional EMT simulations.

The platform for this work will be done in MatLab environment. Models in PSCAD software are assumed to be the most detailed models and will be used as the benchmark models.

1.3 Thesis Outline

The models of the power systems are presented in Chapter 2. It explains the transient stability phenomenon in detail, and discusses traditional approach and the dynamic Phasor based method of modeling the power system in transient stability analysis. The traditional method models the AC network as constant admittance matrix, the generator is modeled without the stator fluxes. For the DP based method, the AC network components are modeled as differential equations using dynamic Phasors; the generator model includes stator fluxes, and the multi-mass turbine system is used to represent

generator rotor. It also discusses the interactions between the AC network model and the generator model.

The SMIB test system is presented in Chapter 3. The AC network components are modeled using dynamic Phasors, and the generator model includes stator fluxes. The DP model will be benchmarked with the traditional transient stability model of neglecting AC network and generator stator dynamics. The model will also be benchmarked with equivalent EMT model to show the validity of the method.

Chapter 4 of this thesis presents the IEEE first benchmark model. The sub-synchronous resonance issue will be discussed. Since the DP model can observe system oscillations in the range up to 60Hz, the sub-synchronous phenomenon can be modeled. The traditional transient stability method would not be able to model this system behavior. The DP model will be compared to equivalent EMT model and traditional model to verify results.

The assessment of the DP model is discussed and summarized in Chapter 5 of this thesis. It includes the main contributions of this research as well as future work this research may benefit to.

CHAPTER 2 MODELS OF THE POWER SYSTEM

2.1 Introduction

The power system is mainly composed of three components, the source, the load, and the transmission system between the source and the load. The interactions between these components become increasingly important in today's deregulated electricity market environment. Power system planning and operation are mainly driven by economy, and the aging power system infrastructures are put under more stressed conditions. The stability of the power system has to be investigated more thoroughly in order to avoid catastrophic events, like the number of blackouts occurred in recent years [3]. This thesis mainly analyzes the transient stability portion of the rotor angle stability of the power system. The proposed method uses the concept of dynamic Phasor in modeling power system AC network components, and includes the stator transients in modeling synchronous generators. This research will prove that the DP method gives more accurate results as compared to traditional modeling approach.

The rotor angle stability is the ability of the power system to regain equilibrium after subject to a severe disturbance [2] [6]. The severe disturbances could include short circuit on a transmission line, loss of a large generator or load, or loss of a tie between two subsystems. The disturbance could cause variations in power transfers, machine rotor speed, bus voltages, and other system variables. The fundamental factor in rotor angle stability is the manner that power outputs of the synchronous machine vary as the

rotor oscillates. The relationship between interchange power and angular positions of the rotors of synchronous machine is non-linear.

In steady state, the mechanical input torque and the electromechanical output torque are in equilibrium for each generator, and rotors of all the machines in the interconnected system are in synchronism. Once disturbed, the rotors of the machines accelerate or decelerate according to the law of motion of a rotating body. It follows the equation of motion as shown in equation (2.1) [8].

$$J\frac{d^2\theta}{dt^2} = T_m - T_e = T_a \tag{2.1}$$

Where,

J	is the total moment of inertia of the rotor mass in kgm^2
T_m	is the mechanical torque supplied by the prime mover in N-m
T_e	is the electrical torque output of the alternator in N-m
Θ	is the angular position of the rotor in rad

The normalized inertia constant H can be expressed as in equation (2.2). The difference in mechanical and electrical torques can be represented in equation (2.3) by combining equations (2.1) and (2.2).

$$H = \frac{Stored\ Kinetic\ Energy\ at\ Synchronous\ Speed\ in\ Mega-Joules}{Generator\ MVA\ Rating} = \frac{J\omega_S^2}{2S_{rated}} \tag{2.2}$$

$$\frac{2HS_{rated}}{\omega_S^2}\frac{d_\theta^2}{d_t^2} = T_m - T_e \tag{2.3}$$

Since power equals to torque times angular velocity, equation (2.3) can be expressed in terms of power as in equation (2.4).

$$\frac{2H}{\omega_s}\frac{d_\theta^2}{d_t^2} = \frac{P_m}{S_{rated}} - \frac{P_e}{S_{rated}} \tag{2.4}$$

Angle θ is the angle which the d-axis leads the axis of phase a as shown in figure 2. Since the rotor is rotating with respect to the stator, angle θ is continuously increasing and is related to the rotor angular velocity ω_r and time as in equation (2.5). Angle θ_0 is the value of θ at time 0, which is δ. In dq frame, angle δ is the angle which the q-axis leads the stator terminal voltage, and it depends on machine loading. It is measured with respect to a reference axis which rotates at synchronous speed. It is more convenient to measure the rotor angular position with respect to a reference axis which rotates at synchronous speed. Therefore, equation (2.4) can be represented in (2.8) by expressing angle θ in terms of angle δ using equations (2.6) and (2.7). The relationships of the rotor angular position as respect to reference frame are represented in figure 3.

$$\theta = \omega_r t + \theta_0 \tag{2.5}$$

$$\frac{d\theta}{dt} = \omega_r + \frac{d\delta}{dt} \tag{2.6}$$

$$\frac{d^2\theta}{dt^2} = \frac{d^2\delta}{dt^2} \tag{2.7}$$

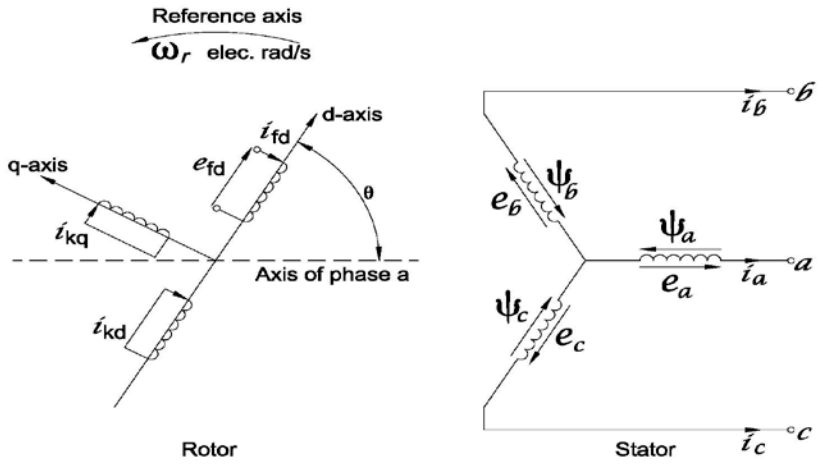

a, b, c	:	Stator phase windings
fd	:	Field winding
kd	:	d-axis amortisseur circuit
kq	:	q-axis amortisseur circuit
k	=	1, 2, … n; n – no. of amotirsseur circuits
Y	=	Angle by which d-axis leads the magnetic axis of phase a winding, electrical rad
ϖr	=	Rotor angular velocity, electrical rad/s

Figure 2 Stator and Rotor Circuits of a Synchronous Machine

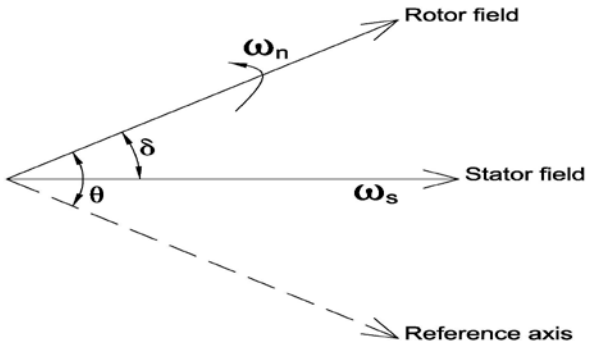

Figure 3 Angular Position of Rotor with Respect to Reference Axis

$$\frac{2H}{\omega_s}\frac{d^2\delta}{dt^2} = P_m - P_e = P_a \quad Per\ Unit \tag{2.8}$$

Equation (2.8) is known as the swing equation, and it represents the dynamic behavior of the rotor.

In terms of the power system, the power angle relationship can be explained using the simple diagram shown in Figure 4. The simple system consists of a synchronous machine and an infinite bus which are connected by a transmission line with reactance X. The synchronous machines can be represented by a model comprised of an internal voltage behind an effective reactance. The power transfer is a function of angular separation (δ), and can be represented by the following equation:

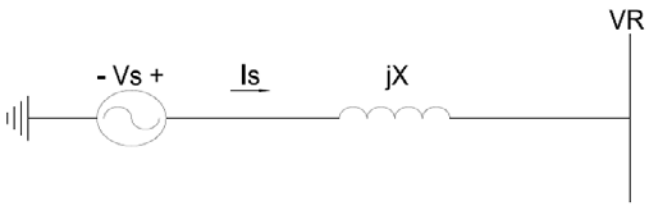

Figure 4 Single Machine Infinite Bus System

$$Pe = \frac{V_1 V_2}{X} \sin \delta \qquad (2.9)$$

Where, Vs=V1∠δ, $V_{R=}V_2$∠0

When the angle is zero, there is no power transfer. As angle increases from 0 to 90^o, the power transfer increases up to the maximum. A further increase in angle results in decrease in power transfer. At angles beyond 90^o, the system becomes transiently unstable. The stability of the system can be analyzed using the Equal Area Criterion (EAC) as shown in Figure 2.2.

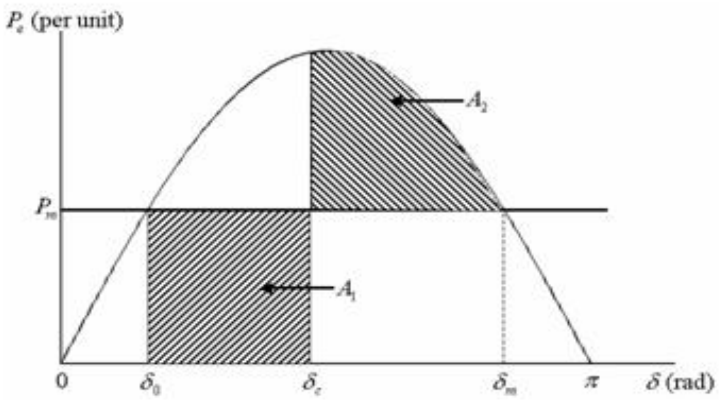

Figure 5 Power Angle Curve for Equal Area Criterion

In steady state, the generator is operating at synchronous speed with rotor angle δ_0, and the electrical output power P_e is equal to mechanical power $P_{m.}$ When a three-phase fault occurs, breakers at both ends of the line will open up to clear the fault. The behavior of the machine rotor follows the EAC as shown in Figure 2.2. The input power is supplied by a prime mover and it is assumed to be constant during the transient period, since the time constant of the turbine mass system is in the order of few seconds and the electrical transients occur in the order of milliseconds. When fault occurs at t = 0 sec, P_e becomes zero suddenly, and P_m remains unchanged. The difference in power causes rotor to accelerate, thus δ increases until the fault is cleared at $t_{c.}$ At the instant of fault clearing, the P_e increases abruptly. Since P_m remains the same, P_e is greater than $P_{m.}$ The difference in P_e and P_m causes rotor angle to decelerate. The area A1 shown in Figure 2.2 is proportional to the increase in kinetic energy of the rotor while it is accelerating, and area A2 shown in Figure 2.2 is proportional to the maximum possible decrease in kinetic energy of the rotor while it is decelerating. Areas A1 must be less than to A2 in order to

restore the rotor to synchronous speed. There is a critical angle for clearing the fault in order to satisfy the requirements of equal-area criterion, and it can be calculated based on the formula shown in equation 2.10.

$$t_{cr} = \sqrt{\frac{4H(\delta_{cr}-\delta_{0)}}{\omega_s P_m}} \qquad (2.10)$$

The detail of application of equal area criterion in response to system faults can be found in reference [6].

In this chapter, the models of the AC network, the generator, and the multi-turbine will be discussed in detail in the following sections.

2.2 AC Network Model

The AC network includes transformers, transmission lines, and static loads. These quantities are represented as constant admittance/impedance calculated at the power frequency (60Hz) for the traditional transient stability studies since transients are assumed to be slow that they are approximated as stationary [1]. This assumption is only valid for slow transients, but not for fast transients. In order to capture transient in the frequency range up to 60Hz, Dynamic Phasors can be used in representing RLC components of the network. The AC network can be represented using combinations of

series RL and parallel RC circuits. The traditional matrix format and the dynamic Phasor representations are presented below.

2.2.1 Network Equations in Admittance Matrix Format

Since the network transients are approximated as stationary in traditional electromechanical studies, the network can be represented as constant admittance matrices. The node admittance matrix can be written as in formula (2.11) below [6].

$$\begin{bmatrix} I_1 \\ \cdots \\ I_n \end{bmatrix} = \begin{bmatrix} Y_{11} & \cdots & Y1n \\ \cdots & \cdots & \cdots \\ Y_{n1} & \cdots & Ynn \end{bmatrix} \begin{bmatrix} V_1 \\ \cdots \\ V_n \end{bmatrix} \qquad (2.11)$$

Where,

N	total number of nodes
Y_{ii}	self admittance of node i
Y_{ij}	mutual admittance between nodes i and j
V_i	Phasor voltage to ground at node i
I_i	Phasor current flowing into the network at node i

This formulation includes the effect of static loads. The elements of the matrix are constant except for changes introduced by network switching operations. The effects of generators, nonlinear static loads, dynamic loads, and other devices are reflected by boundary conditions with additional V and I relationships.

For simulation of faults, the elements of the admittance matrix can be changed to reflect different type of faults.

2.2.2 Dynamic Phasor Representation

The constant admittance network representation in a transient stability model can reasonably approximate power system oscillations up to 5Hz. For oscillations above 5Hz, network transients and generator stator dynamics have to be modeled to obtain more accurate results. Time varying Dynamic Phasors have been shown to be able to formulate linear differential equations for the fast transients in the lumped RLC network irrespective of the transient speed [12]. The time varying Phasors are Fourier coefficient series with the higher order coefficients truncated, leaving only those significant series [16]. This thesis will use Dynamic Phasor to model the transient stability phenomenon by representing the AC network using Dynamic Phasors, and to capture transients up to 60HZ.

The dynamic Phasor in RI frame can be derived as follows.

Consider a sinusoidal signal in the form of equations (2.12) and (2.13) below.

$$v(t) = V_t\,(\cos(\omega_o t + \delta(t)) + j\sin(\omega_o t + \delta(t))) \qquad (2.12)$$

Where, V_t is the magnitude of the voltage, and $\delta(t)$ is the phase of the voltage.

$$v(t) = V_t\,(\cos(\delta(t)) + j\sin(\delta(t)))e^{j\omega_o t} \qquad (2.13)$$

Let $V_R = V_t(\cos(\delta(t)))$, and $V_I = V_t\,(\sin(\delta(t)))$, then equation 2.13 can be written in the rectangular coordinates.

$$\bar{v}(t) = (V_R + jV_I)e^{j\omega_o t} \quad (2.14)$$

The oscillatory frequencies generated by the dynamic devices are included on the Phasor voltage V_R and V_I. The capacitors and inductors of the network can be represented using these time varying Phasors. Most of the components in the AC network can be represented as the combination of series RL and parallel RC circuits.

During faults, the series RL and parallel RC circuits can be represented by updating new voltage and current values.

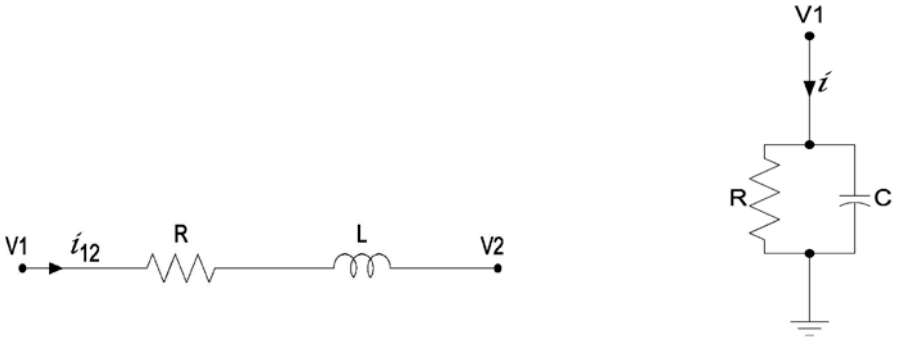

(a) **(b)**

Figure 6 (a) Series RL Circuit (b) Parallel RC Circuit

2.2.2.1 Series RL Circuits

Referring to figure 6 (a), the instantaneous voltage across nodes 1 and 2 can be represented by equation (2.15). The instantaneous voltage is a time varying signal, and frequency independent.

$$v_{12} = L\frac{di_{12}}{dt} + Ri_{12} \quad (2.15)$$

Equation (2.15) can be re-written as equation (2.16) in Phasor format

$$(V_R + jV_I)e^{j\omega_0 t} = L\frac{d(I_{12R}+jI_{12I})e^{j\omega_0 t}}{dt} + R(I_{12R}+jI_{12I})e^{j\omega_0 t} \quad (2.16)$$

After differentiation using the product rule, equation (2.16) can be written as follows. The time varying dynamic Phasor representation depends on the fundamental frequency ω_0. Phasors are not instantaneous current and voltage quantities; they are time varying RMS quantities of fundamental frequency.

$$V_R + jV_I = L\frac{d(I_{12R}+jI_{12I})}{dt} + (R + j\omega_0)(I_{12R} + jI_{12I}) \quad (2.17)$$

Equation 2.17 can be separated into real and imaginary parts as shown in equations 2.18 and 2.19 respectively.

$$\frac{d}{dt}(I_{12R}) = \frac{1}{L}(V1_R - V2_R - RI_{12R}) + \omega 0(I_{12I}) \quad (2.18)$$

$$\frac{d}{dt}(I_{12I}) = \frac{1}{L}(V1_I - V2_I - RI_{12I}) - \omega 0(I_{12R}) \quad (2.19)$$

2.2.1.2 Parallel RC Circuits

The instantaneous current flowing from node 1 to ground in figure 6 (b) can be represented by equation (2.20) below.

$$i_{12} = C\frac{dv_1}{dt} + Rv_1 \tag{2.20}$$

Equation (2.18) can be re-written as equation (2.19) in Phasor format

$$(I_R + jI_I)e^{j\omega_0 t} = C\frac{d(V_{1R}+jV_{1I})e^{j\omega_0 t}}{dt} + R(V_{1R}+jV_{1I})e^{j\omega_0 t} \tag{2.21}$$

After differentiation using the product rule, equation (2.22) can be written as follows. The real and imaginary parts of equation (2.22) are shown in equations (2.23) and (2.24) respectively.

$$I_R + jI_I = C\frac{d(V_{1R}+jV_{1I})}{dt} + (R + j\omega_0)(V_{1R} + jV_{1I}) \tag{2.22}$$

$$\frac{d}{dt}(V_{1R}) = \frac{1}{C}I_R - RV_{1R} + \omega 0 V_{1I} \tag{2.23}$$

$$\frac{d}{dt}(V_{1I}) = \frac{1}{C}I_I - RV_{1I} - \omega 0 V_{1R} \tag{2.24}$$

2.3 Generator Model

In conventional transient studies, generator stator flux is modeled as differential equations, and the stator transients are neglected. There are two main reasons for making these assumptions. One reason is to have consistency in terms of number of equations in representing various elements of the power system. For stability studies involving slow variations having frequencies below 5Hz, network transients do not have to be modeled since they decay rapidly. In order to neglect network transients, generator transients have to be neglected too. The other reason is to simplify computation complexity and to reduce computation speed. The stator transients in dq frame are represented by the $d/dt\varphi_d$ and $d/dt\varphi_q$ terms in the transformer voltage equations (2.25) and (2.26). The $d/dt\varphi_d$ and $d/dt\varphi_q$ terms prevent $\varphi_{d\ and}$ φ_q from changing instantaneously, and result in dc offset in the phase currents. The analysis with both fundamental frequency and unidirectional components of phase currents included would be complex and computationally costly. By eliminating these terms, the unidirectional or dc offset components and its associated dynamic performance can be removed. The $\varphi_{d\ and}$ φ_q are assumed to change instantly following a disturbance. The speed variations ω_r is assumed to be constant to counterbalance the effect of neglecting stator transients [6].

$$e_d = \frac{d}{dt}\varphi_d - \omega_r\varphi_q - R_a i_d \quad (2.25)$$

$$e_q = \frac{d}{dt}\varphi_q + \omega_r\varphi_d - R_a i_q \quad (2.26)$$

With damper windings, the synchronous generators are modeled either as 6th order (round rotor type) or 5th order (salient pole rotor type). The detailed derivation of the generator equations can be found in [6].

For this thesis, the generators are modeled as 8th order, and there are 2 q axes. The synchronous generators in dq frame can be represented using equations (2.27) to (2.32) [6]. This model includes damper windings.

$$\frac{d}{dt}\varphi fd = \omega 0\ [efd - \frac{Rfd}{Lfd} + \frac{Rfd}{Lfd}L"ads(-id + \frac{\varphi fd}{Lfd} + \frac{\varphi 1d}{L1d})] \quad (2.27)$$

$$\frac{d}{dt}\varphi 1d = \omega 0[-\frac{R1d}{L1d}\varphi 1d + \frac{R1d}{L1d}L"ads(-id + \frac{\varphi fd}{Lfd} + \frac{\varphi 1d}{L1d})] \quad (2.28)$$

$$\frac{d}{dt}\varphi 1q = \omega 0[-\frac{R1q}{L1q}\varphi 1q + \frac{R1q}{L1q}L"aqs(-iq + \frac{\varphi 1q}{L1q} + \frac{\varphi 1q}{L1q})] \quad (2.29)$$

$$\frac{d}{dt}\varphi 2q = \omega 0[-\frac{R2q}{L2q}\varphi 2q + \frac{R2q}{L2q}L"aqs(-iq + \frac{\varphi 2q}{L2q} + \frac{\varphi 2q}{L2q})] \quad (2.30)$$

$$\frac{d}{dt}\Delta\omega r = \frac{1}{2H}(Tm - \varphi diq + \varphi qid - kD\Delta\omega r) \quad (2.31)$$

$$\frac{d}{dt}\delta = \Delta\omega r * \omega 0 \quad (2.32)$$

In order to capture the fast dynamics in the frequency range between 5Hz and 60Hz, the stator fluxes of the d and q axis are included in the generator model, and equations (2.33) and (2.34) are added to the generator model. The speed ω_r is a time varying variable, not a constant quantity [5] [6].

$$\frac{d}{dt}\varphi d = (ed + (\frac{\Delta\omega r * \omega 0 + \omega 0}{\omega 0})\varphi q + Raid) \quad (2.33)$$

$$\frac{d}{dt}\varphi q = (eq - (\frac{\Delta\omega r * \omega 0 + \omega 0}{\omega 0})\varphi d + Raiq) \quad (2.34)$$

The 8th order generator model will be used in conjunction with the dynamic Phasor AC network model to capture fast transients of the power system.

2.4 Multi-Mass Turbine Model

In terms of analyzing dynamic response of the power system, most models consider the rotor of the turbine generator as a single mass. The frequency of modes of oscillation is below 2Hz. In reality, the rotor of the turbine generator is made up by a multi-mass connected by shafts of finite stiffness. Torsional oscillations can result between different sections of the turbine-generator rotor. The frequencies of these oscillations are in the sub-synchronous range. The subsynchronous frequency is the difference between the synchronous frequency and the natural torsional frequency. If the subsynchronous frequency is close to the natural frequency of the power system, adverse effects could occur. This includes problems with power system controls, subsynchronous resonance issue with series capacitor-compensated transmission lines, and torsional fatigue duty due to network switching [7][27]. The thesis will mainly model the subsynchronous resonance issue with series capacitor-compensated transmission lines.

In order to analyze subsynchronous oscillations, stator transients and network transients have to be modeled which are neglected in standard transient stability programs. In this thesis, the generator will be modeled with stator transients and the AC

network will be modeled using dynamic phasor representations as described in previous sections of this chapter.

A typical multi-mass model of a generator unit is shown in Figure 7. The five torsional masses include rotors of the generator, low-pressure (LP) turbine sections, intermediate-pressure (IP) turbine sections and High-pressure (HP) turbine sections.

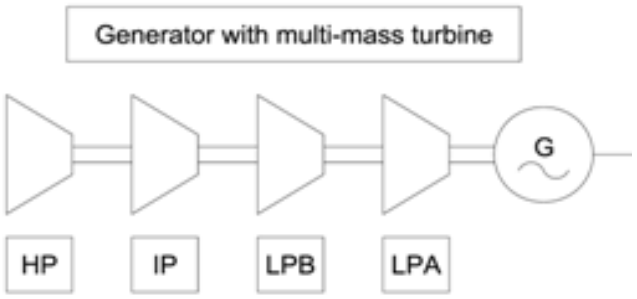

Figure 7 Model of a Typical Multi-mass Shaft System

The dynamic characteristics of the shaft system are defined mainly by three sets of parameters: inertia constant H of each mass, torsional stiffness K of shaft sections connecting adjacent masses, and damping coefficient D associated with each mass. The equations for H and K are presented in equations (2.2) and (2.31) respectively.

$$K = \frac{GF}{l} = \frac{G}{l}\left(\frac{\pi d^4}{32}\right) \tag{2.31}$$

Where,

G = rigidity modulus of shaft material
F=form factor which defines the geometric property
l=length of shaft

The torque transmitted is proportional to the torsional stiffness K and the angular twist θ by equation (2.32).

$$T = K\theta \tag{2.32}$$

For each individual section of the multi-mass turbine-generator system, the accelerating torque T_a is defined by the equations of motion shown in equations (2.33) and (2.34). Ta is also the difference between input torque (T_{in}) and output (T_{out}) and damping (T_D) torques as in equation (2.35).

$$2H_1 \frac{d}{dt}\Delta\omega r = Ta \tag{2.33}$$

$$\frac{d}{dt}\delta = (\Delta\omega r)\omega 0 \tag{2.34}$$

$$T_a = T_{in} - T_{out} - T_D \tag{2.35}$$

The complete set of equations for the rotor system of five torsional masses shown in Figure 7 is represented in equations (2.36) to (2.45).

Generator: $\frac{d}{dt}\Delta\omega r1 = \frac{1}{2H1}(K12(\delta 2 - \delta 1) - \ edid + \ eqiq - D1\Delta\omega r1)$ (2.36)

$$\frac{d}{dt}\delta 1 = \Delta\omega r1 * \omega 0 \tag{2.37}$$

LP_A: $\frac{d}{dt}\Delta\omega r2 = \frac{1}{2H2}(Tlpb + K23(\delta 3 - \delta 2) - K12(\delta 2 - \delta 1) - D2\Delta\omega r2)$ (2.38)

$$\frac{d}{dt}\delta 2 = \Delta\omega r2 * \omega 0 \tag{2.39}$$

LP_B: $\frac{d}{dt}\Delta\omega r3 = \frac{1}{2H3}(Tlpa + K34(\delta 4 - \delta 3) - K23(\delta 3 - \delta 2) - D3\Delta\omega r3)$ (2.40)

$$\frac{d}{dt}\delta 3 = \Delta\omega r3 * \omega 0 \quad (2.41)$$

IP: $$\frac{d}{dt}\Delta\omega r4 = \frac{1}{2H4}(Tip + K45(\delta 5 - \delta 4) - K34(\delta 4 - \delta 3) - D4\Delta\omega r4) \quad (2.42)$$

$$\frac{d}{dt}\delta 4 = \Delta\omega r4 * \omega 0 \quad (2.43)$$

HP: $$\frac{d}{dt}\Delta\omega r5 = \frac{1}{2H5}(Thp - K45(\delta 5 - \delta 4) - D5\Delta\omega r5) \quad (2.44)$$

$$\frac{d}{dt}\delta 5 = \Delta\omega r5 * \omega 0 \quad (2.45)$$

2.5 Combining Generator Model and Network Components

The generator models explained previously are represented in dq frame and the AC network components are represented in RI frame. In order to combine the generator model and the AC network components, the generator terminal voltages and currents have to be converted from RI frame to dq frame, and verse visa using the conversion matrix S.

$$[S] = \begin{bmatrix} cos\delta & sin\delta \\ sin\delta & -cos\delta \end{bmatrix} \quad (2.5.1)$$

$$\begin{bmatrix} e_q \\ e_d \end{bmatrix} = [S]\begin{bmatrix} E_R \\ E_I \end{bmatrix} \quad (2.5.2)$$

$$\begin{bmatrix} E_R \\ E_I \end{bmatrix} = [S]^{-1}\begin{bmatrix} e_q \\ e_d \end{bmatrix} \quad (2.5.3)$$

The changes in the d q components of the machine terminal current can be represented by the following formulas.

$$i_d = K_{id3b}\varphi_d + K_{id4b}\varphi_{fd} + K_{id5b}\varphi_{1d} \quad (2.5.4)$$

$$i_q = K_{iq6b}\varphi_q + K_{iq7b}\varphi_{1q} + K_{iq8b}\varphi_{2q} \quad (2.5.5)$$

Where,

$$L_{adpp} = \frac{1}{(\frac{1}{L_{ad}} + \frac{1}{L_{fd}} + \frac{1}{L_{1d}})}$$

$$K_{id3b} = \frac{-1}{(L_1 + L_{adpp})}$$

$$K_{id4b} = \frac{L_{adpp}}{(L_1 + L_{adpp})L_{fd}}$$

$$K_{id5b} = \frac{L_{adpp}}{(L_1 + L_{adpp})L_{1d}}$$

$$L_{aqpp} = \frac{1}{(\frac{1}{L_{aq}} + \frac{1}{L_{1q}} + \frac{1}{L_{2q}})}$$

$$K_{iq6b} = \frac{-1}{(L_1 + L_{aqpp})}$$

$$K_{id7b} = \frac{L_{aqpp}}{(L_1 + L_{aqpp})L_{1q}}$$

$$K_{id8b} = \frac{L_{aqpp}}{(L_1 + L_{aqpp})L_{2q}}$$

CHAPTER 3 SINGLE MACHINE INFINITE BUS SYSTEM

3.1 Introduction

As mentioned previously, stator winding dynamics and dynamic representation of the AC network components are essential in representing high frequency (> 5Hz) oscillations in transient stability studies. This thesis proposes a model that includes stator winding dynamics and AC network dynamics, which can be used for low frequency electromechanical oscillations and high frequency interactions.

The main purpose of this single machine infinite bus system (SMIB) is to prove that the Dynamic Phasor model can be used to analyze low frequency oscillations. In this test system, only low frequency oscillations (<5Hz) can be produced by the interaction between the generator and the AC network.

The proposed dynamic phasor model will be compared with two models: traditional technique which ignores stator winding dynamics and represent AC network components using constant admittance/impedance, and EMT equivalent model. The electromagnetic transient simulation results from EMT model are used as the benchmark for the comparison.

3.2 Proposed Test Model

A SMIB system shown in figure 8 below is used as the test system. The system is based on the system taken from the textbook: Power System Stability and Control [6]. In order to model the system using dynamic Phasors, shunt capacitances are added to the two parallel transmission lines. This model is mainly used to validate the proposed method with low frequency oscillations (<5Hz).

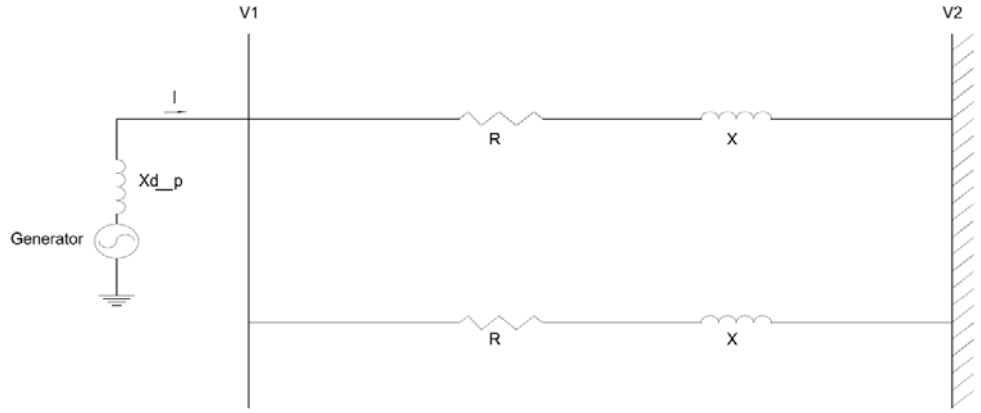

Figure 8 Single Machine Infinite Bus Model

The generator is the 8th order model which includes damper windings and stator dynamics as explained in chapter 2. The two transmission lines are modeled with the combinations of series RL and parallel RC circuits. The state equations are derived based on the method described in the AC dynamic network section 2.2 of this thesis. All the current and voltage equations include both a real and an imaginary component. The series RL equations and the parallel RC equations are shown in Appendix A of this these.

The combination of the two currents in the series RL component (I) is considered as the current injected to the dynamic AC network model from the generator. The d q components of I in terms of stator and rotor fluxes are represented by equations (2.5.4) and (2.5.5).

In order to verify the transient stability method, a three phase fault is applied at the middle of one of the parallel transmission lines. The network during fault is shown in Figure 9. During the fault, the generator equations remain the same since there is no change in generator model. In terms of AC network equations, the parallel RC circuit remains the same during the fault, and the series RL circuit of the faulted transmission line is modified to reflect the fault.

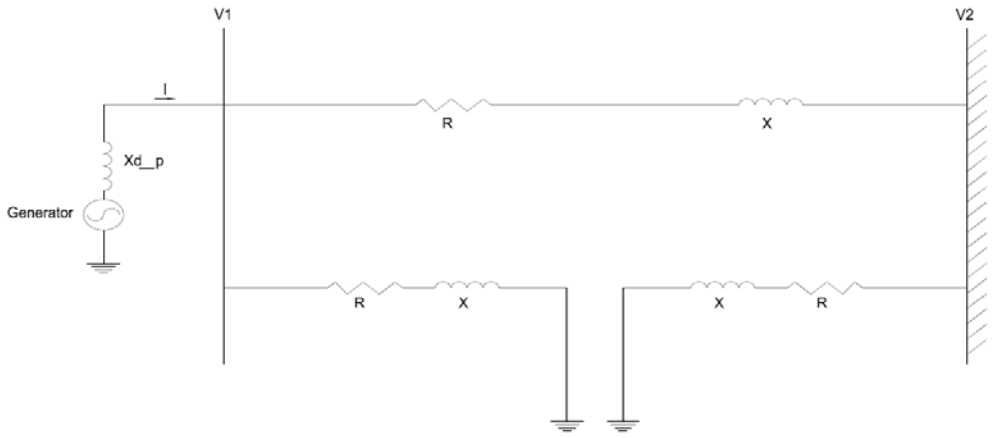

Figure 9 Single Machine Infinite Bus Model with 3 Phase Fault at Middle of the Second Transmission Line

Post the fault, breakers at the end of the line are open to isolate the fault as shown in Figure 10. The AC network has been changed to one transmission line, and the modified current and voltage equations of the network are modified to reflect the change.

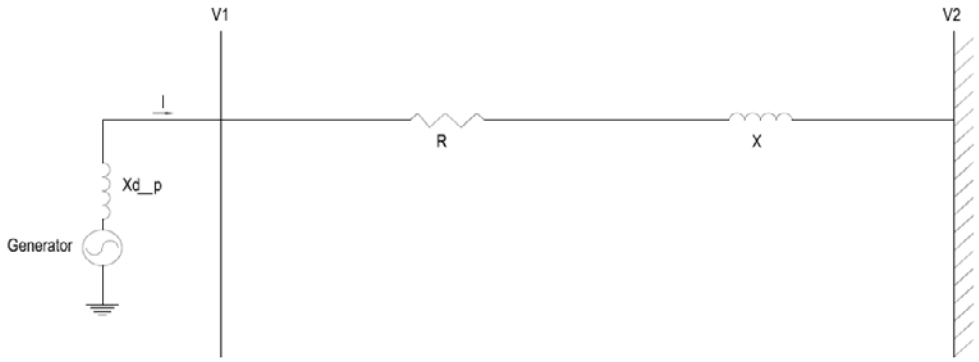

Figure 10 Single Machine Infinite Bus Model with 3 Phase Fault Removed

3.3 Validation of the Dynamic Phasor Model

Transient responses of the Dynamic Phasor model for the disturbance applied are compared to the traditional model and detailed EMT model. The Dynamic Phasor model is programmed in MatLab environment, and the integration method used is RK4.

A three phase fault was applied to middle of one of the parallel transmission lines at 2.0 seconds, and the fault was removed at 2.02 seconds, thus, the fault clearing time is 0.02 seconds. The simulation was run for 20 seconds, and the rotor speed and rotor angle were measured as a function of time. There were no damping applied to the generator model. The simulation results were compared between the three models.

In terms of oscillations, the dynamic Phasor model, the traditional method and EMT model give very similar results at low frequency. In this case, the frequency oscillation is approximately 1.312Hz. The simulation results are shown in Figures 11 to 13. The simulation results indicate that the system is transiently stable after subjected to the disturbance at the specified fault clearing times. For Figures 13 and 14, the magnitudes of the spike for dynamic Phasor model are much higher than EMT model

when fault was applied. This has to be addressed in future work. Most likely a smooth signal is required to reduce the magnitude in DP model.

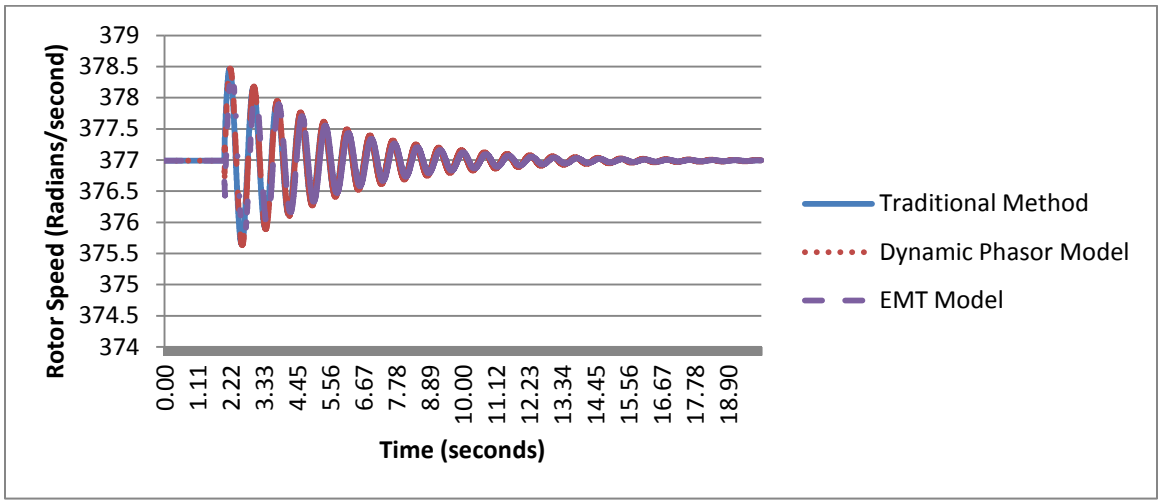

Figure 11 Comparison of Response of the Rotor Speed between Traditional Method, Dynamic Phasor, and EMT Models

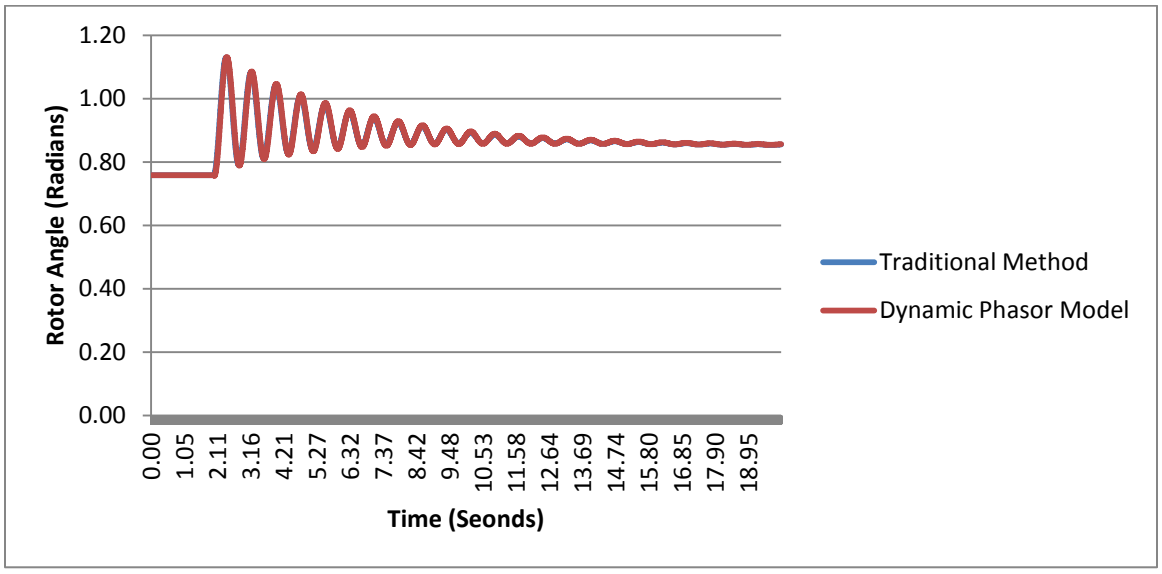

Figure 12 Comparison of Rotor Angle Response between Traditional Method, Dynamic Phasor and EMT Models

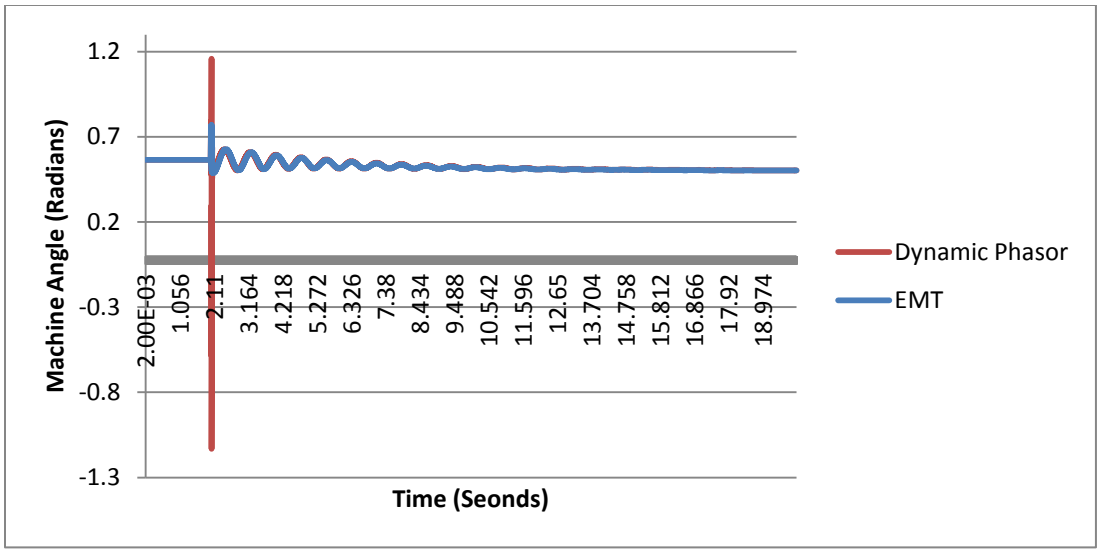

Figure 13 Comparison of Machine Angle Response between Dynamic Phasor and EMT Models

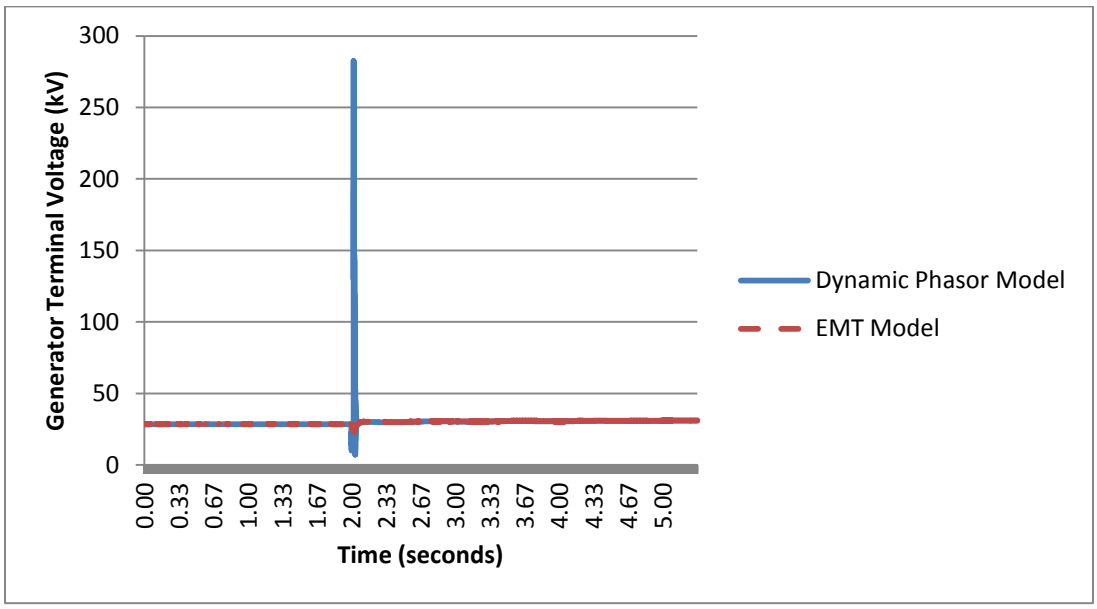

Figure 14 Comparison of Generator Terminal Voltage Response between Traditional Method, Dynamic Phasor and EMT Models

In conclusion, the Dynamic Phasor model gives accurate results for low frequency oscillations. The results obtained from the DP are similar to the traditional modeling method and the EMT simulation results.

3.4 Time Steps

The time step is also of interests for this research. It is compared between Dynamic Phasor model and the detailed EMT model.

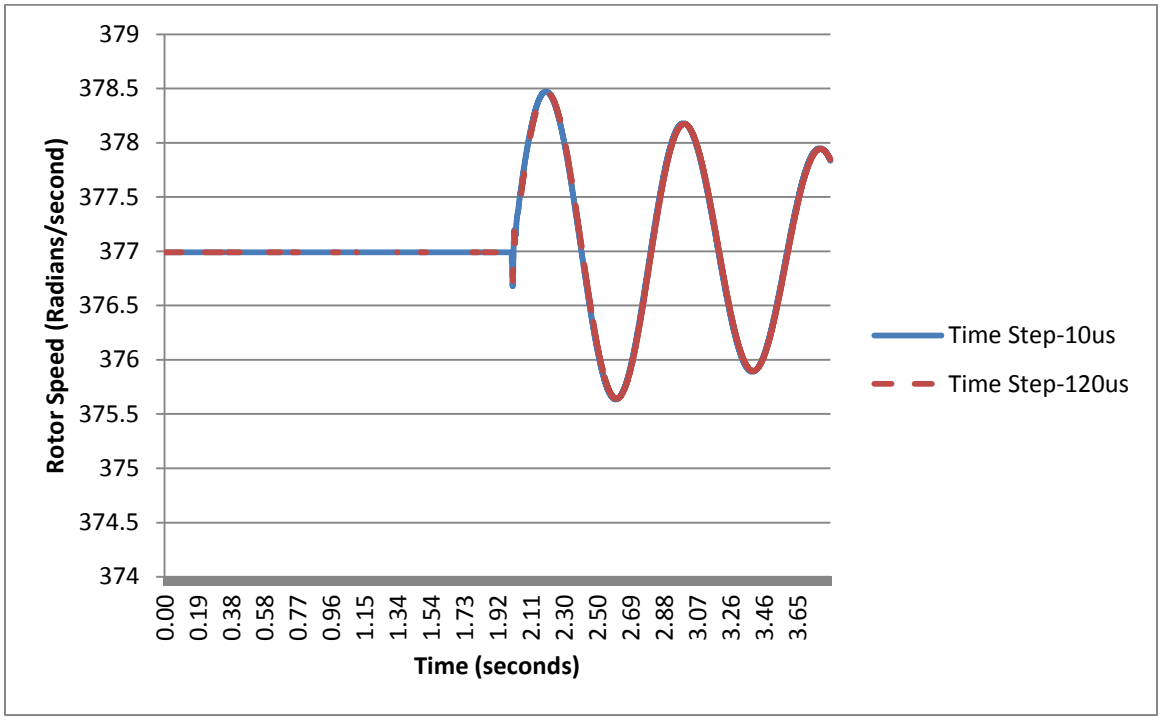

Figure 15 Comparison of Change in Generator Speed at Various Time Steps for DP Model

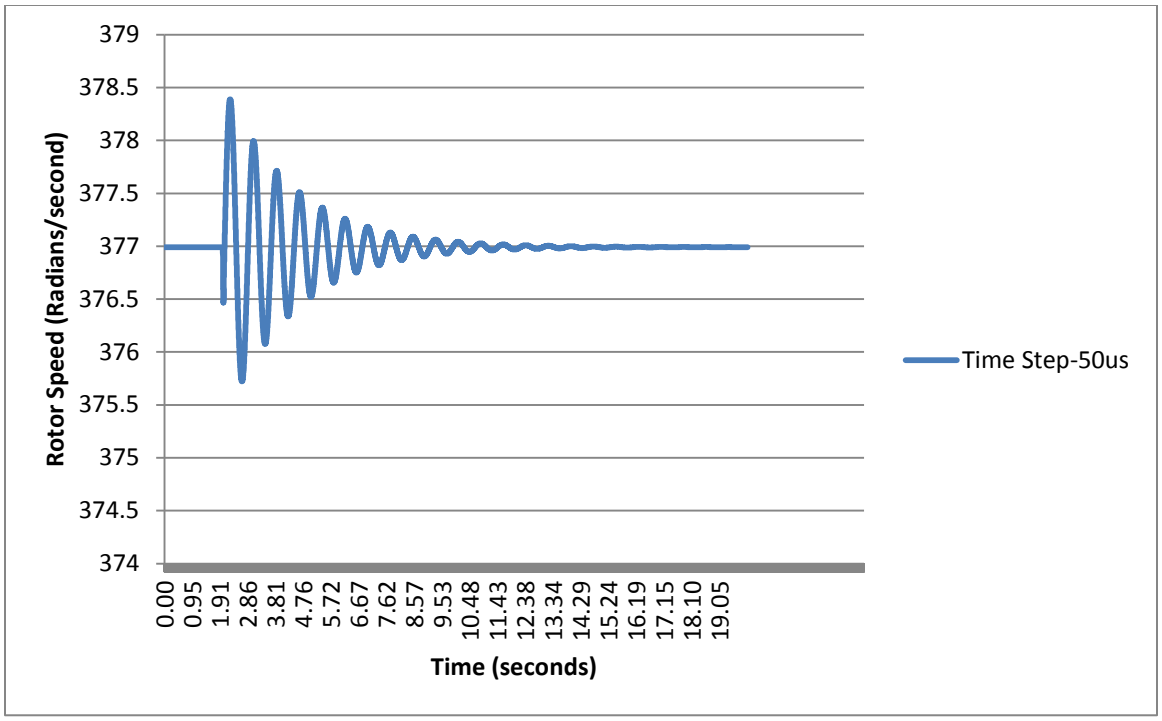

Figure 16 Change in Generator Speed at 50us Time Step for EMT Model

The time steps used in the Dynamic Phasor model gives accurate results for up to 120μs as compared to typical PSCAD/EMTDC simulation of 50μs. The proposed model offers some advantage in terms of time step, approximately twice as large as the detailed model. The plots are shown in Figure 3.6 and 3.7 for dynamic Phasor model and for PSCAD/EMTDC model respectively.

3.5 Conclusions

In this chapter, the proposed dynamic phasor model suitable for analyzing low frequency transient stability studies is presented in detail. The model is validated to give accurate results in the low frequency (<5Hz) range.

The model is tested on a SMIB system, and a 3 phase fault is applied to the system and cleared after 0.02 seconds by removing the faulted line. The responses of the generator speed, rotor angle, and generator terminal voltage are compared between the DP model, the traditional transient stability model and the EMT models. The results indicate very close match between all three models in all the variables investigated, thus, the proposed dynamic Phasor model is very accurate in representing low frequency oscillations (there are no high frequency oscillation in this test model).

The time step size is also investigated between the DP model and detailed EMT model. The dynamic Phasor model shows an advantage of 2 times bigger than EMT model using RK4 integration technique. This time step can be further improved with better integration methods, such as trapezoidal and improved RK4. Since the main objective of this thesis is to prove that the proposed Dynamic Phasor model can be used for low and high frequency oscillation, other integration techniques will not be investigated here.

In conclusion, the Dynamic Phasor model is accurate in analyzing low frequency oscillations and it offers advantage of a larger time step as compared to detailed EMT model.

CHAPTER 4 GENERATOR TURBINE TORSIONAL INTERACTION

4.1 Introduction

Generator rotor is considered as a single mass for typical transient stability programs. It actually consists of multiple mass connected by shafts of different stiffness. Torsional oscillation could result between different sections of the generator-turbine rotor if the generator is disturbed. The oscillation in the sub-synchronous range could cause resonance with the electrical system, and this thesis mainly deals with issues in this frequency range.

The phenomenon of sub-synchronous resonance (SSR) mainly occurs in series capacitor compensated transmission system. It can cause either self-excitation due to induction generator effect and interactions with torsional oscillations. This thesis mainly deals with torsional interactions, and the phenomenon is explained in the following sections.

If the complement of the nominal frequency (ω_n) of the network is close to one of the torsional frequencies of the turbine-shaft system, torsional oscillation can be excited. The complement of the natural frequency is the difference between synchronous frequency (ω_0) and natural frequency. This could cause growing oscillations and shaft torque with high magnitude, and could cause damage to the generator or the turbine shaft if these oscillation modes are not sufficiently damped.

Since SSR issue mainly deals with energy interchange between the generator shaft system and the LC components of the transmission network, the electromechanical dynamics of the generating units and the network have to be represented in order to accurately model the phenomenon. Currently, only electrometrical transient programs, such as EMTP and PSCAD/EMTDC can be used to perform time domain analysis of issues of this nature. The limitation it has is the time step since EMT program is expected to be accurate up to very high frequencies (several thousand Hz). The time step has to be sufficiently small to give accurate results; therefore, only small system can be represented.

The Dynamic Phasor model includes the stator dynamics of the generator and the LC dynamics of the transmission network, and it intends to cover frequencies up to nominal frequency. This thesis will prove that the DP model can accurately model the SSR phenomenon without using small time steps, thus, a large system can be simulated.

The IEEE first benchmark model for sub-synchronous resonance is used as the test system for the proposed model [23]. The system is shown in Figure 16. The generator is modeled with multi-mass turbine-generator system as described in Section 2.4 of this thesis. The AC network is modeled using Dynamic Phasors as presented in Section 2.2 of this thesis.

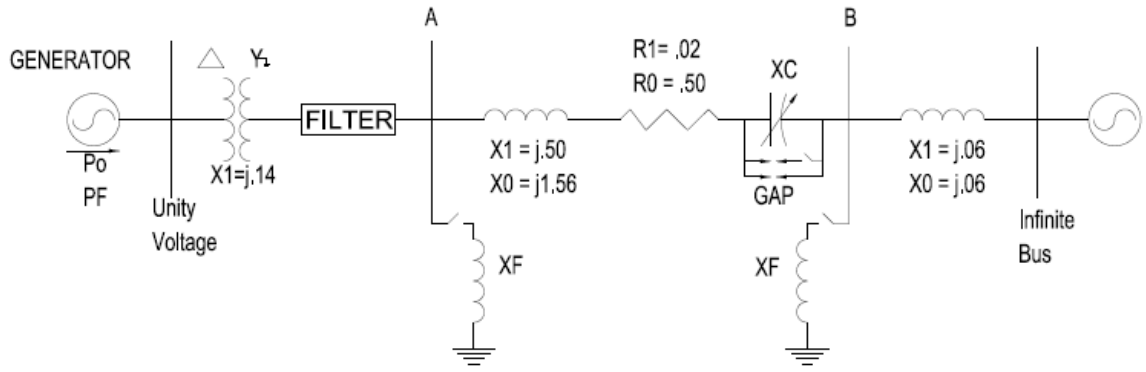

Figure 17 IEEE First Benchmark Model for Sub-synchronous Resonance Studies

4.2 Proposed Test Model

The IEEE first benchmark model is modified to model using Dynamic Phasor to represent the transmission system. The modified system is shown in Figure 17 below.

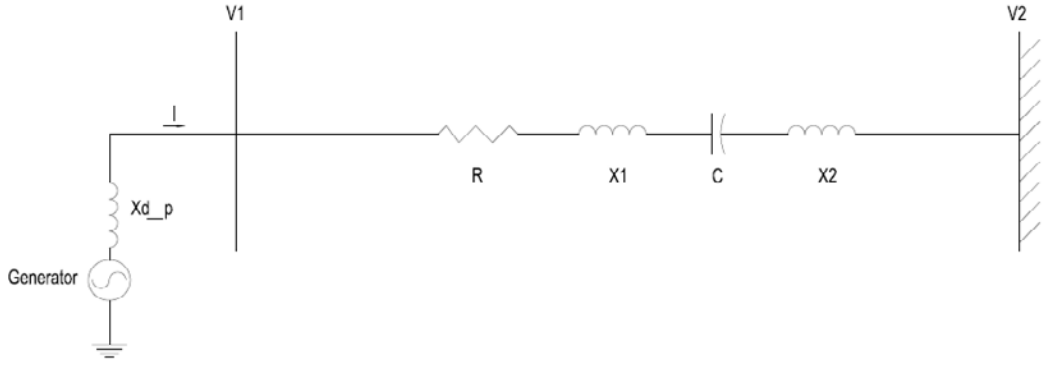

Figure 18 Modified IEEE First Benchmark Model for Dynamic Phasor Model

The rotor is modeled as a multi-mass system with 4 turbines and a generator component. The modeling detail of the multi-mass turbine system can be found in section 2.4 of thesis. The transmission system consists of a series RLC circuit, and shunt capacitances are added to the transmission line. The transformer reactance is added to

the generator reactance to simplify modeling. It is reduced from 0.14pu to 0.001pu to make reasonable generator reactance value in EMT model, thus, the same value are used in DP model and constant admittance/impedance model. The static exciter is not modeled. All the generator-turbine and the AC network parameters are given or derived from the data given in the IEEE First Benchmark Model for Computer Simulation of Sub-synchronous resonance [23]. The test system with detailed turbine models is represented in Figure 18.

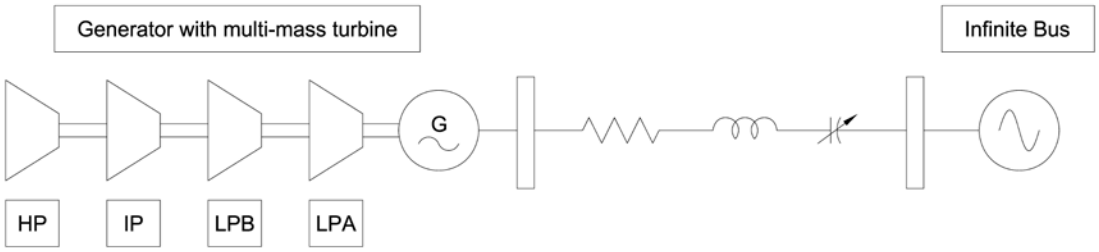

Figure 19 Test System Model with Detailed Multi-mass Turbine System

In total, the test system consists of 26 state variables: generator and shaft system (18), and the AC network (8). It includes the following details:

- Synchronous generator model including stator dynamics,
- A four-mass turbine model consisting of HP, IP, LPB and LPA sections,
- The AC network model using Dynamic Phasors.

The accuracy of the model will be benchmarked with equivalent EMT model using time domain simulations.

4.3 Validation of the Proposed Dynamic Model

The proposed model using Dynamic Phasor was benchmarked with EMT equivalent model and equivalent constant admittance network model. A small disturbance was applied to the infinite bus voltage by reducing the voltage to 95% of its nominal value for 0.075 seconds. The generator rotor speed and generator terminal voltage were compared to EMT simulations and constant admittance/impedance network model. The level of line compensation used for the comparison is 48%.

The comparison plots of change in generator rotor speed and generator terminal voltage between the Dynamic Phasor model and the EMT simulations are shown in Figures 19, 20, 21 and 22 respectively. All the high frequency oscillations in the sub-synchronous range show a very close match to EMT results. These results verify that the Dynamic Phasor model can accurately represent the sub-synchronous oscillations in the system. It can be used to analyze these oscillations in the transient stability assessment.

The change in generator rotor angle between the Dynamic Phasor model and the constant admittance model is shown in Figure 23. The frequency of oscillation in this case is 16Hz, which is in the sub-synchronous frequency range. The DP model shows all the high frequency oscillations in the sub-synchronous range, whereas the traditional constant admittance model cannot capture the oscillation of interests. This is due to simplification of the generator model when modeling constant admittance, the stator dynamics are ignored and the speed variation is assumed to be constant. The results show that the Dynamic Phasor model can be used to study oscillations in the sub-synchronous frequency range.

In conclusion, the Dynamic Phasor model gives very accurate results for high frequency oscillation in the sub-synchronous frequency range. The accuracy of the model will be further investigated in the following section with various line compensation levels.

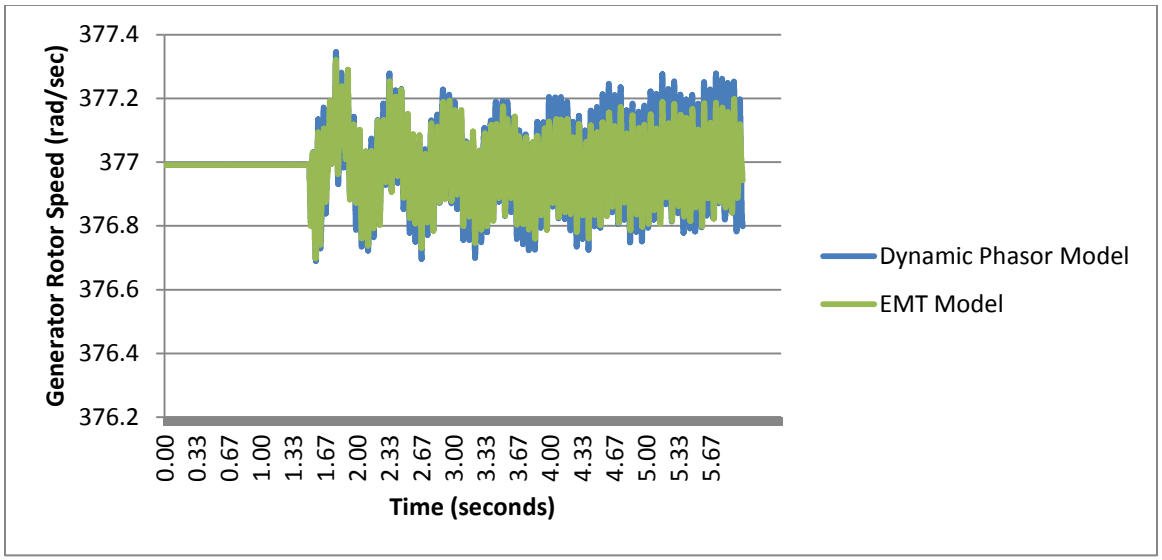

Figure 20 Change in Generator Speed when Line Compensation is 48%

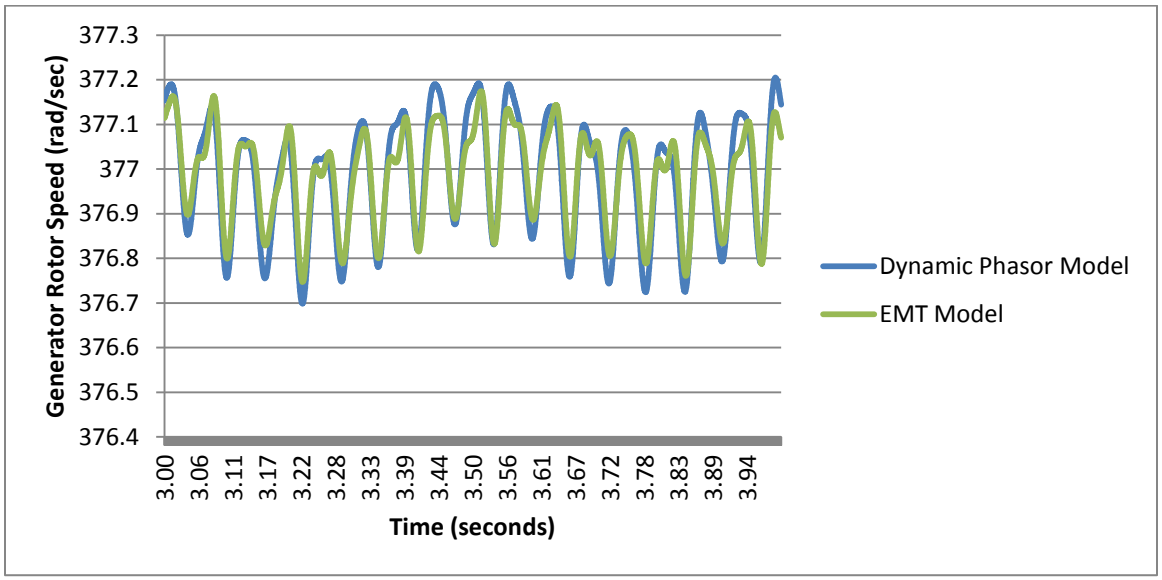

Figure 21 Change in Generator Speed when Line Compensation is 48% (Zoomed in Plot)

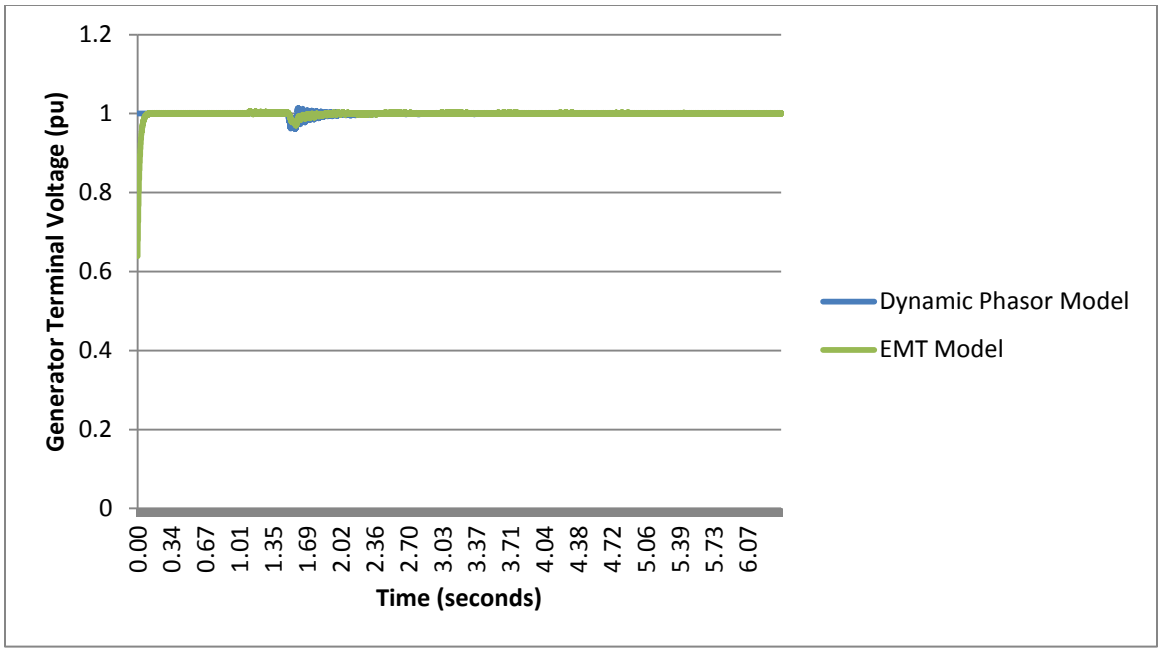

Figure 22 Change in Generator Terminal Voltage when Line Compensation is 48%

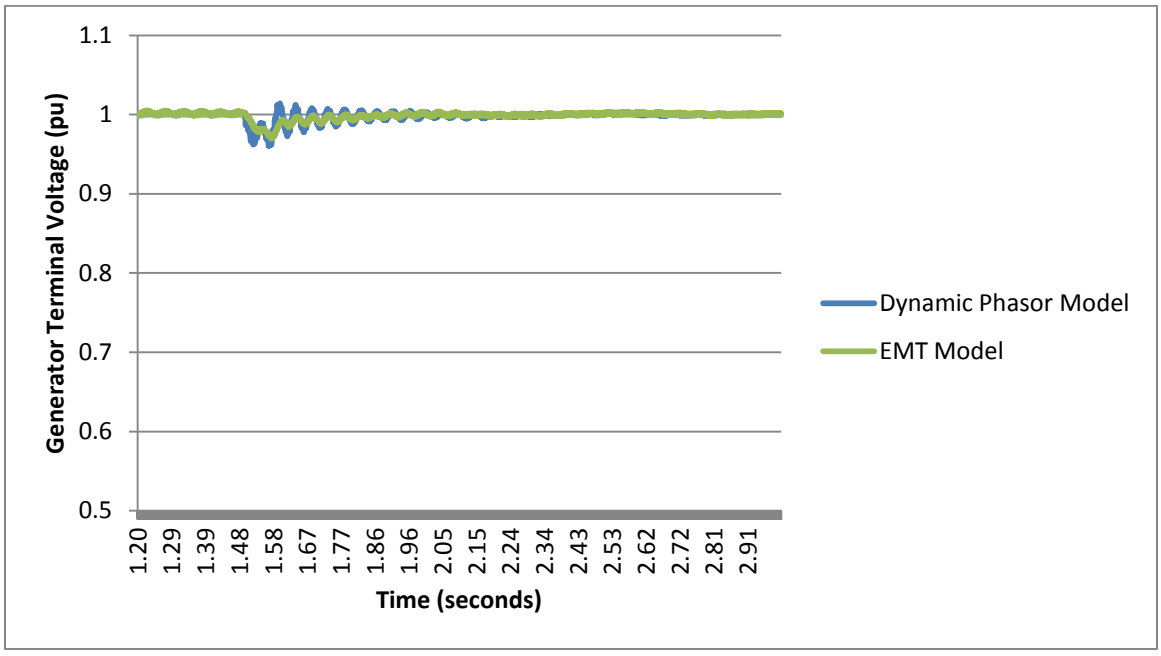

Figure 23 Change in Generator Terminal Voltage when Line Compensation is 48% (zoomed in)

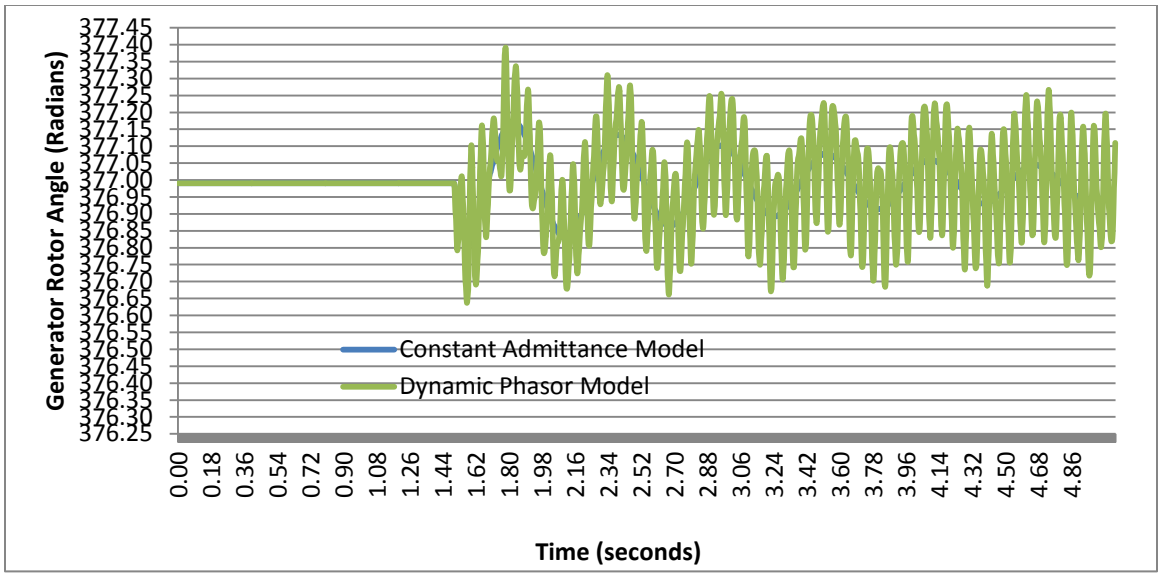

Figure 24 Comparison of Change in Generator Speed between Dynamic Phasor Model and Constant Admittance Model

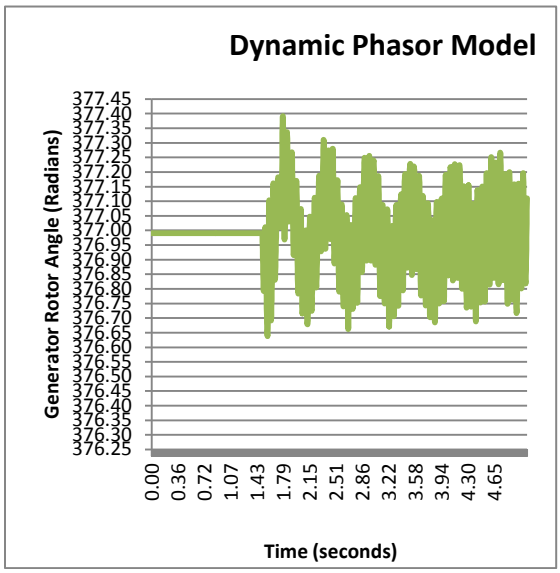

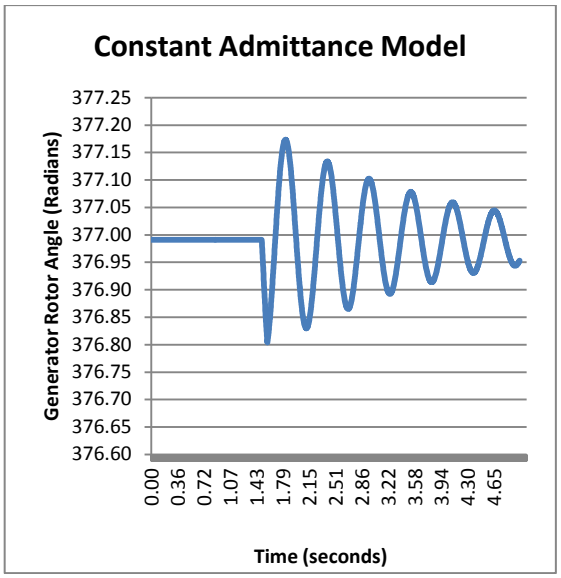

4.4 Analysis at Various Line Compensation Levels

In a series capacitor compensated transmission system, the torsional interactions highly depend on the level of line compensation of the transmission line. The capacitor value of the proposed model is varied to generate line compensation levels from 6% to 70% to investigate torsional interactions, and to further validate the Dynamic Phasor model with detailed EMT model.

The results at 6%, 16%, 36%, and 56% line compensations are presented in Figures 24 through 33 respectively. Mainly 16Hz and 32Hz oscillations are observed from the plots. For Figures 31 and 32, both the DP model and EMT model show stable results. The only difference is the magnitude between the two models, the DP model shows a higher magnitude than the EMT model.

The results show very close match between the Dynamic Phasor model and the detailed EMT model.

In conclusion, the Dynamic Phasor model gives reasonably accurate results as compared to EMT model. It can be used for analysis of sub-synchronous frequency oscillations.

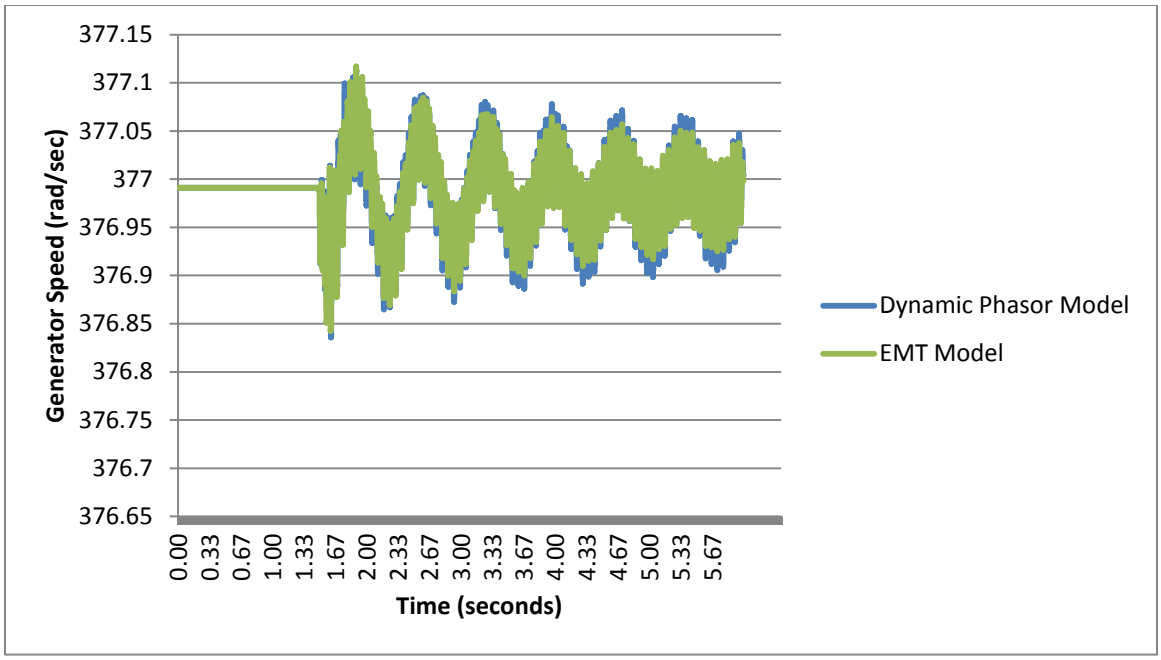

Figure 25 Change in Generator Speed when Line Compensation is 6%

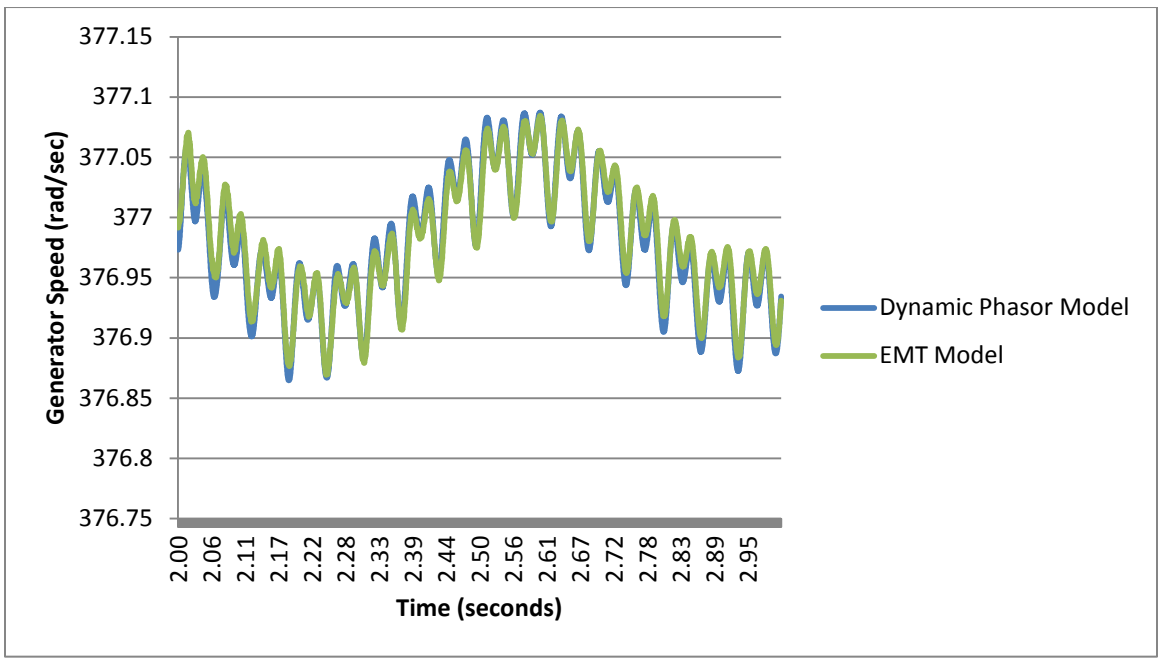

Figure 26 Change in Generator Speed when Line Compensation is 6% (zoomed in plot)

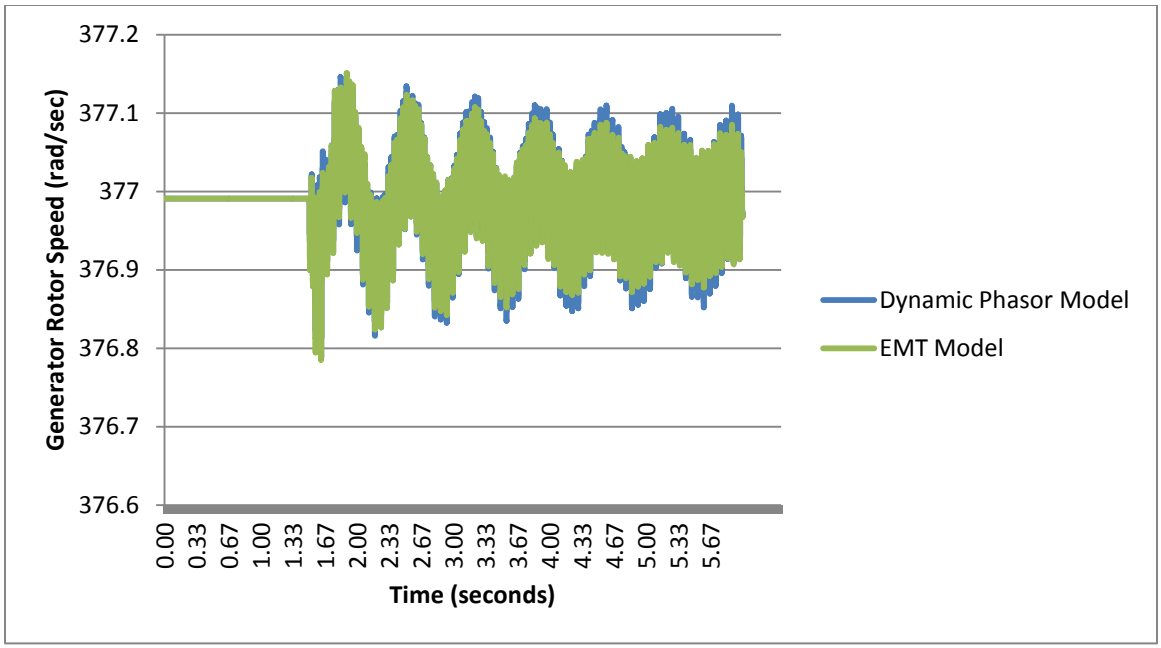

Figure 27 Change in Generator Speed when Line Compensation is 16%

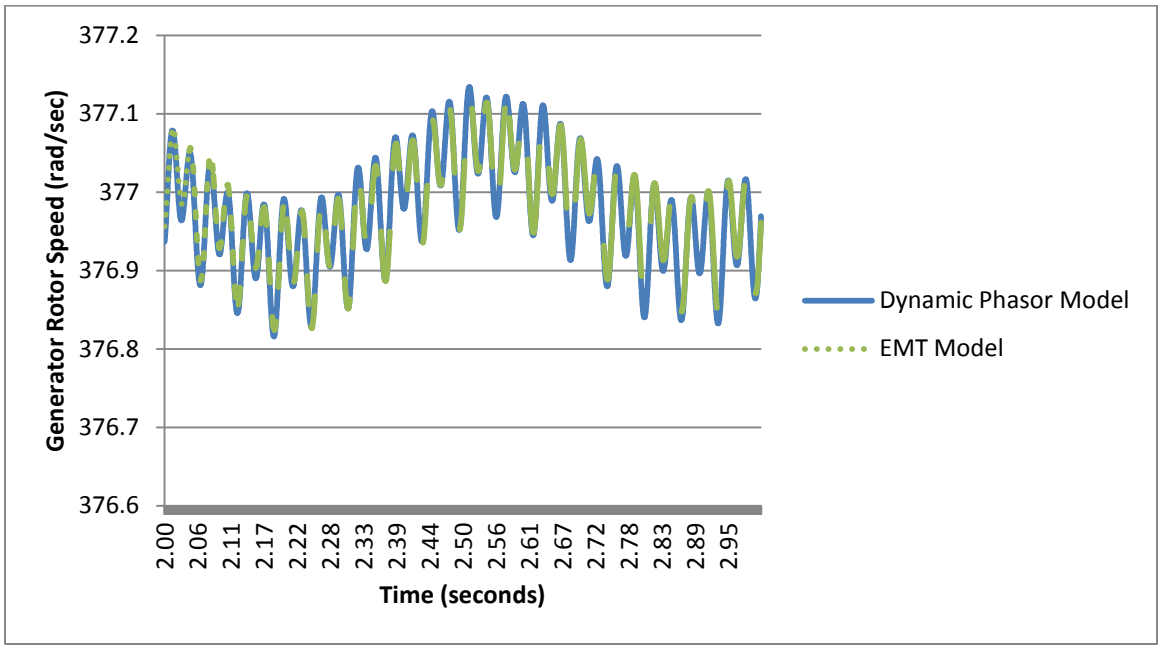

Figure 28 Change in Generator Speed when Line Compensation is 16% (zoomed in)

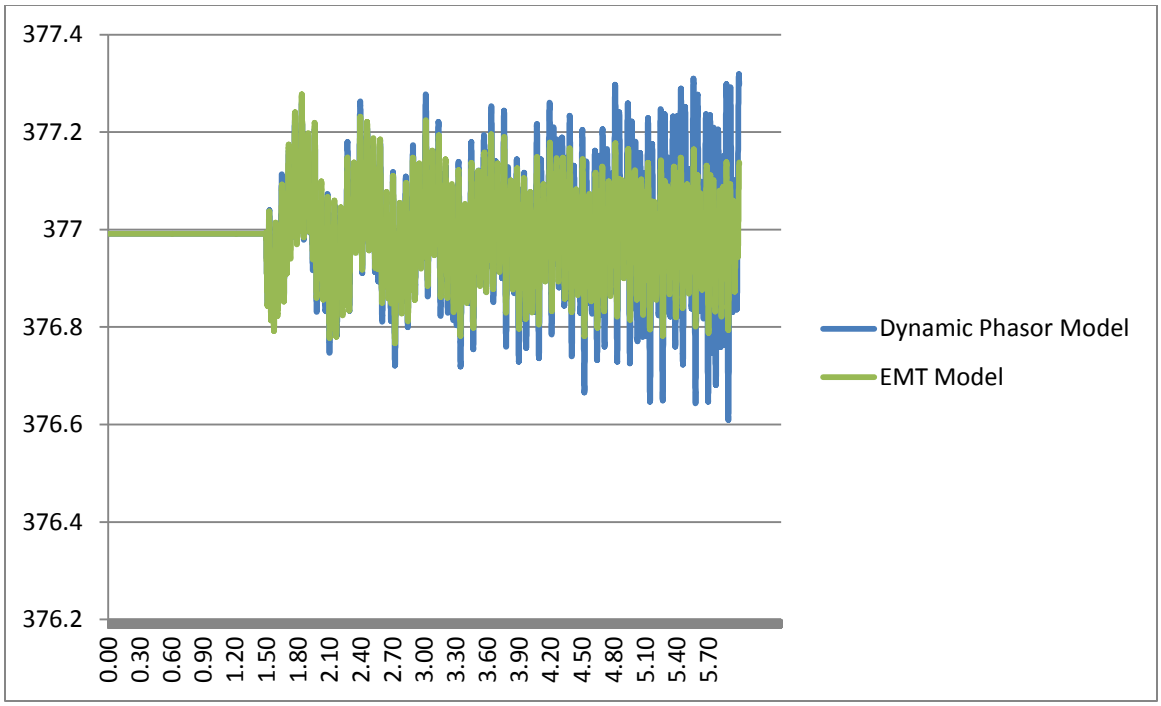

Figure 29 Change in Generator Speed when Line Compensation is 36%

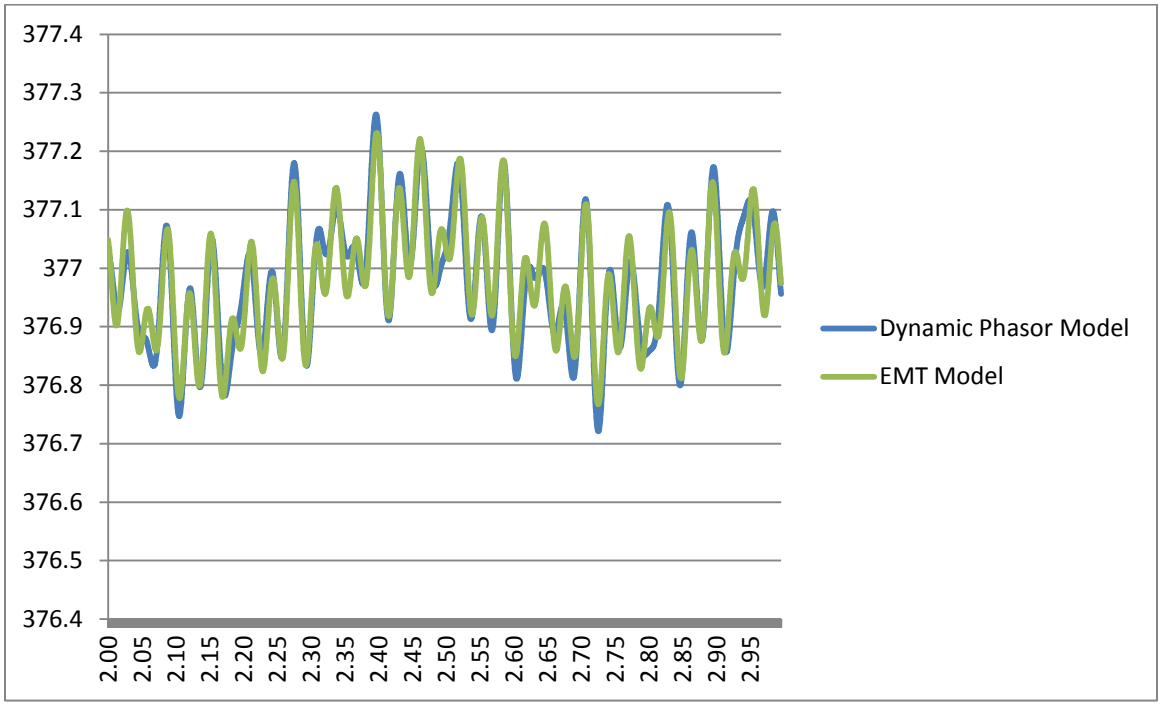

Figure 30 Change in Generator Speed when Line Compensation is 36% (zoomed in plot)

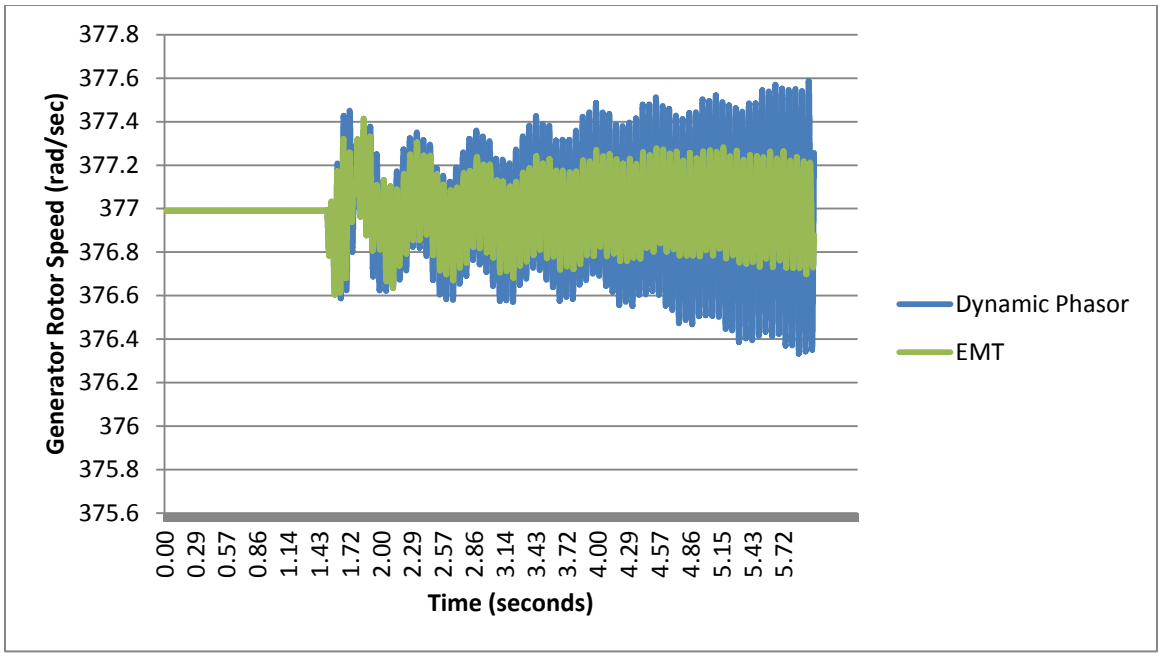

Figure 31 Change in Generator Speed when Line Compensation is 56%

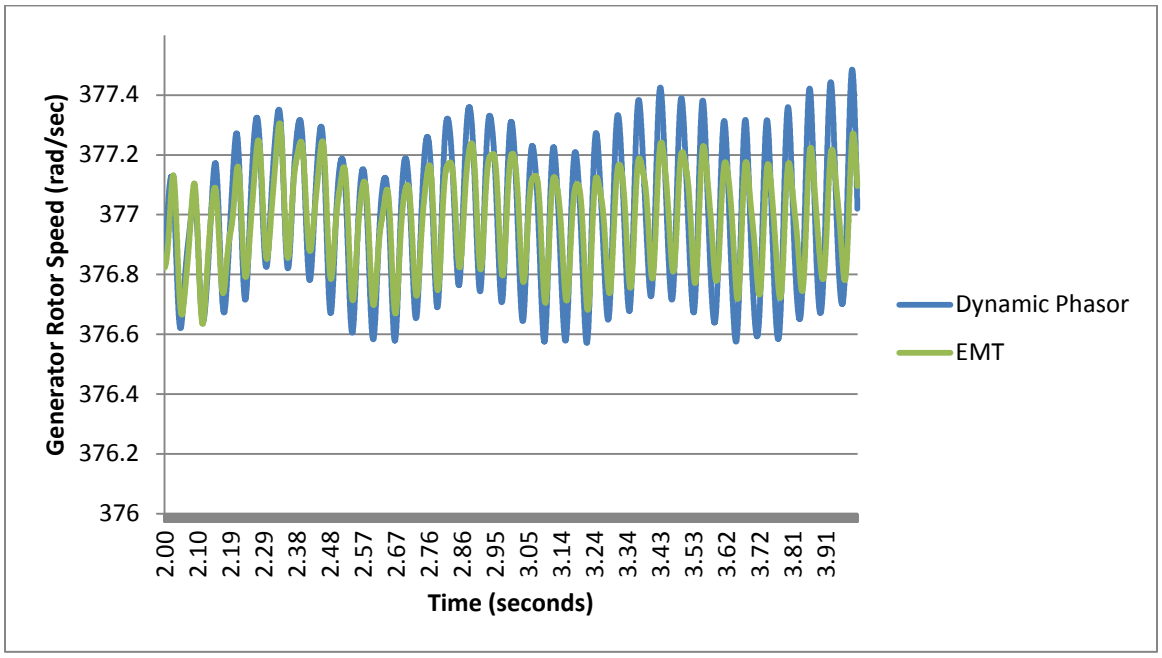

Figure 32 Change in Generator Speed when Line Compensation is 56% (zoomed in)

4.5 Time Steps

One objective of this research is to prove that the DP model can be simulated using larger time steps as compared to the conventional EMT simulations. This is significant in terms of modeling large power systems.

The simulations were tested for the proposed model at various time steps to find the maximum time step without causing numerical errors. The small disturbance was applied by reducing infinite bus voltage to 95% of its nominal value. The change in generator rotor speed was simulated using 10μs, 600μs and 670μs time steps for the proposed model with line compensation of 16%. The simulation results are shown in Figures 34, 35, 36 and 37. The results are similar for up to 660μs as compared to 10μs simulation. Numerical error occurs at approximately 670μs time step.

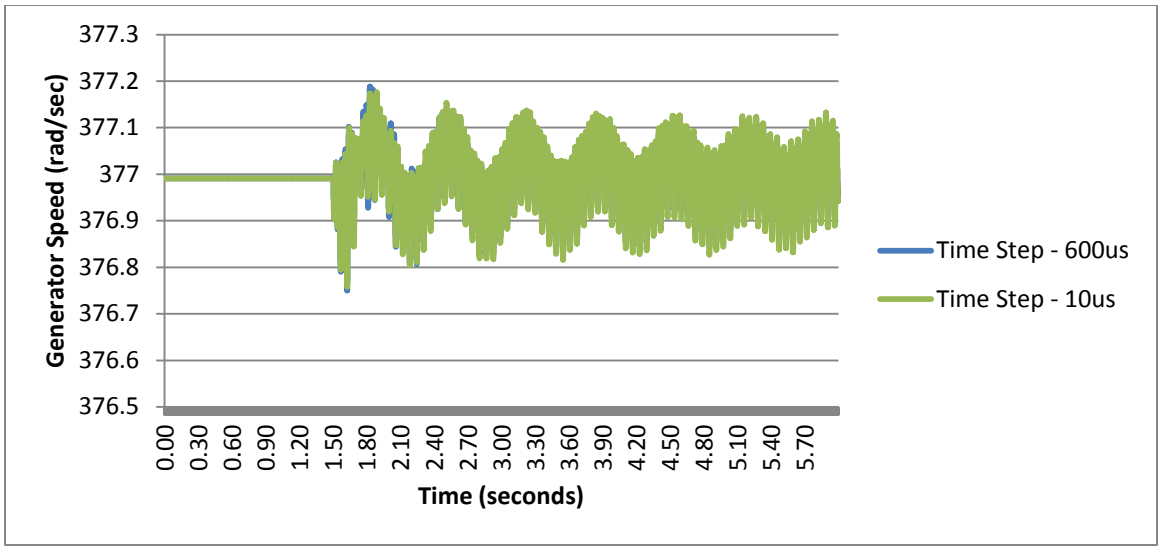

Figure 33 Comparison of Change in Generator Speed for Dynamic Phasor Model at 600us and 10us Time Steps

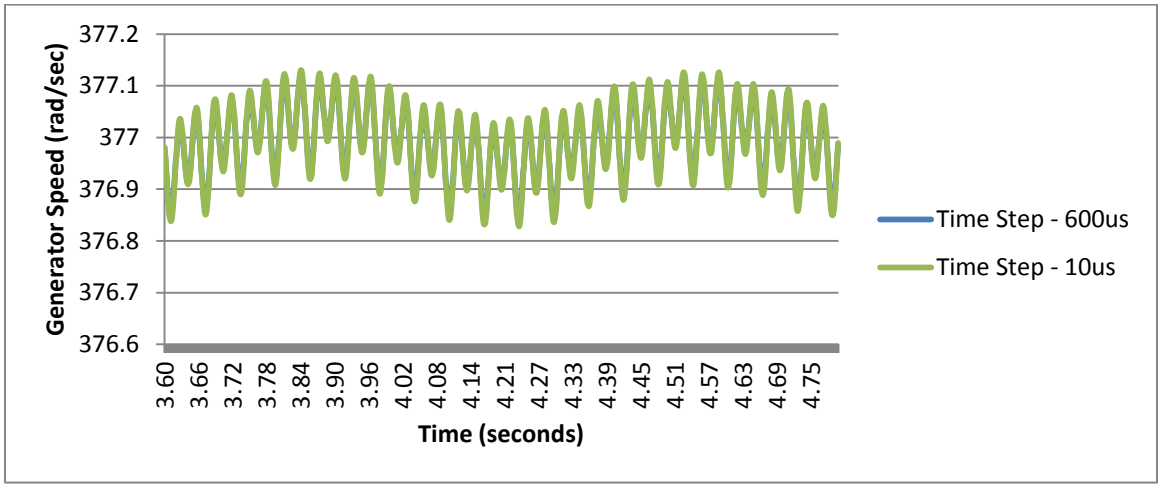

Figure 34 Comparison of Change in Generator Speed for Dynamic Phasor Model at 600us and 10us Time Steps (zoomed in)

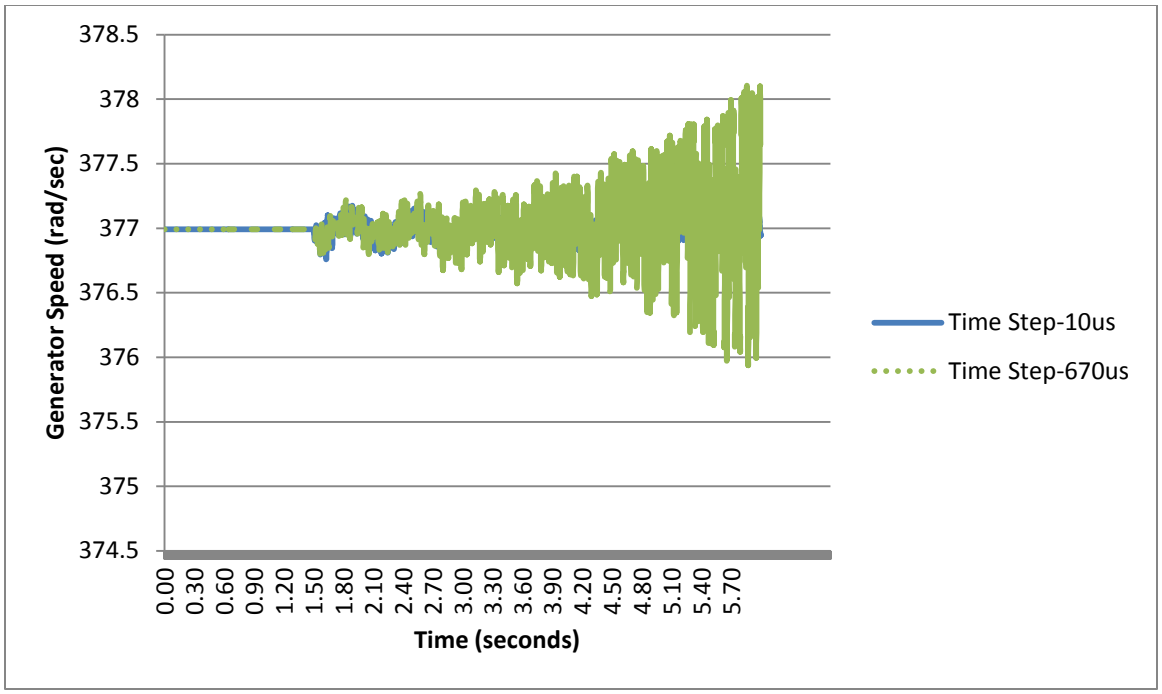

Figure 35 Comparison of Change in Generator Speed for Dynamic Phasor Model at 670us and 10us Time Steps

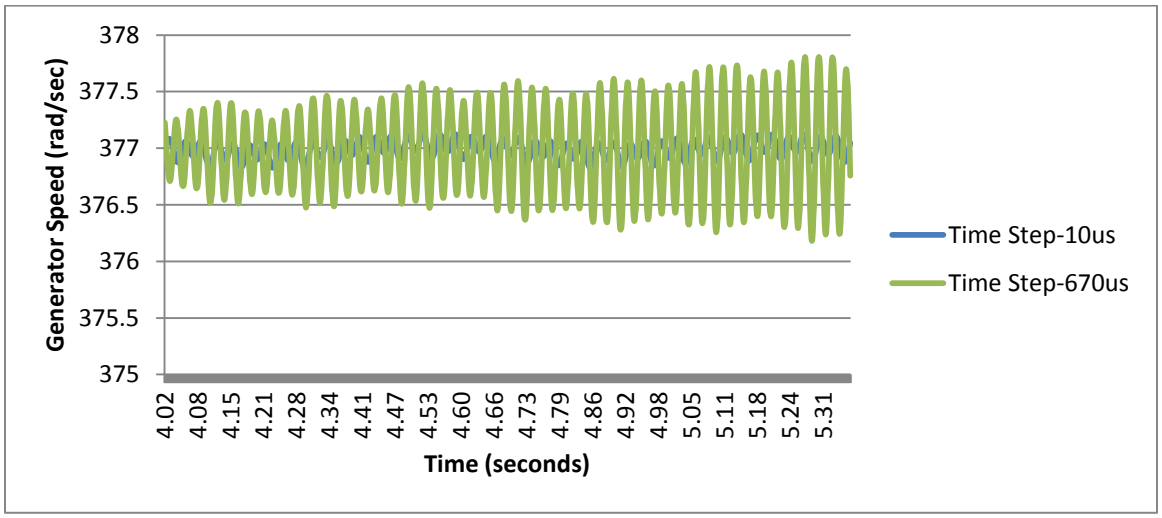

Figure 36 Comparison of Change in Generator Speed for Dynamic Phasor Model at 670us and 10us Time Steps (zoomed in)

The time step size is also investigated in detailed EMT simulations with the same disturbance applied and the generator speed is measured. The results are compared between 10μs and 20μs, and 10μs and 23μs time step simulation runs. They are shown in

Figures 38, 39 and 40 respectively. It can be observed that the results at 10μs and 20μs matched closely, but results are significantly different between 10μs and 23μs. Therefore, EMT simulations can give accurate results for up to 20μs time step in terms of analyzing sub-synchronous resonance oscillations. The time step in EMT model is highly dependent on the time constant or period in the circuit, and approximately 10% of the smallest time constant in the circuit determines the maximum time step required for accuracy. The time step required in the circuit of interest is approximately 13μs (6.0832 Ω time 21.66μF). The 20μs time step requirement is very close to the theoretical value of 13μs.

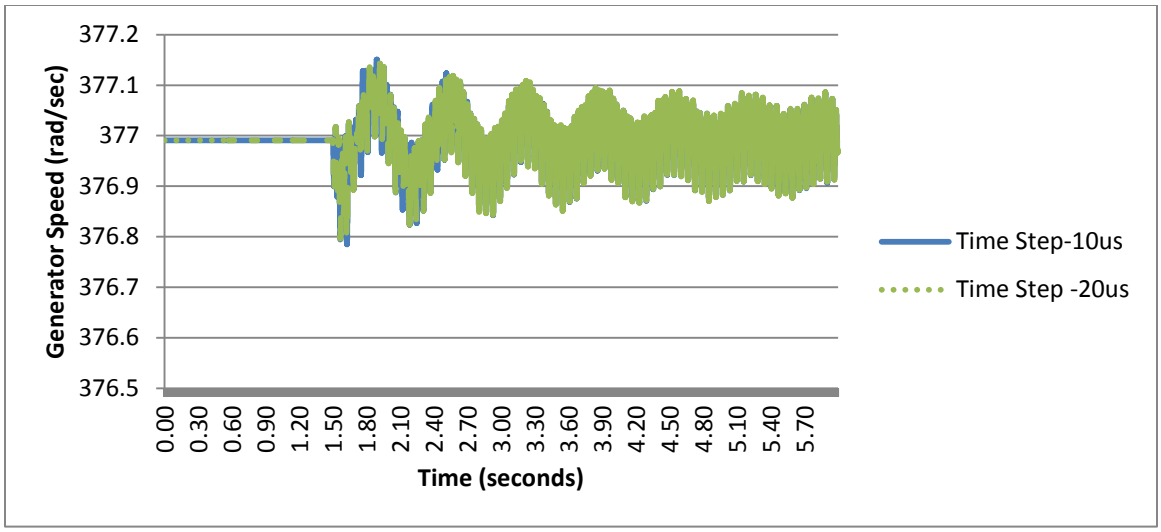

Figure 37 Changes in Generator Speed at Time Steps of 10us and 20us for EMT Model

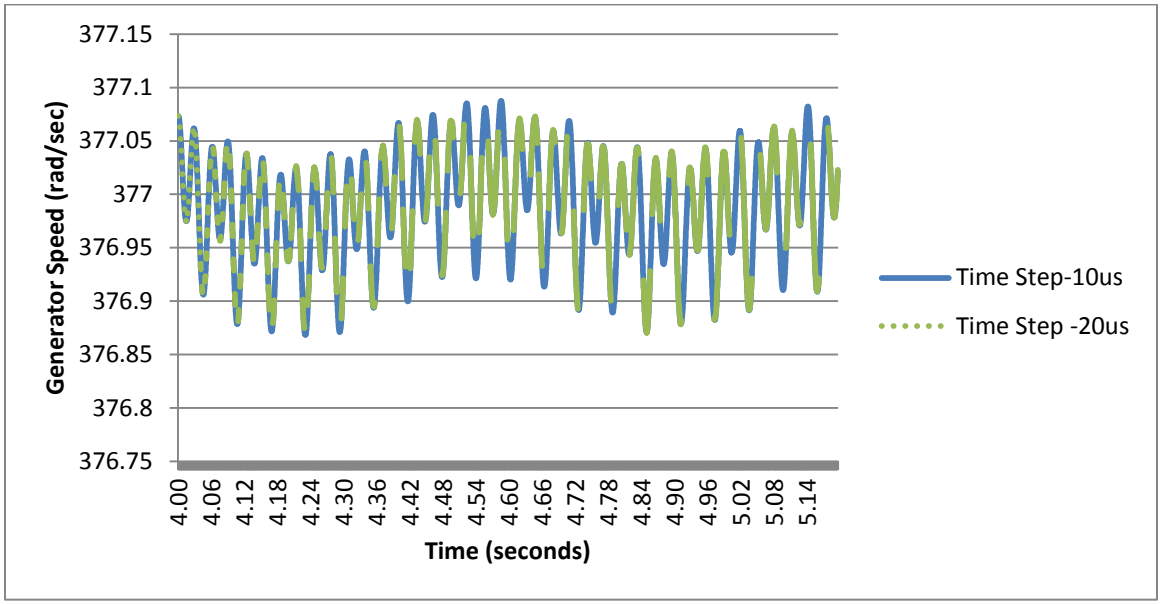

Figure 38 Changes in Generator Speed at Time Steps of 10us and 20us for EMT Model

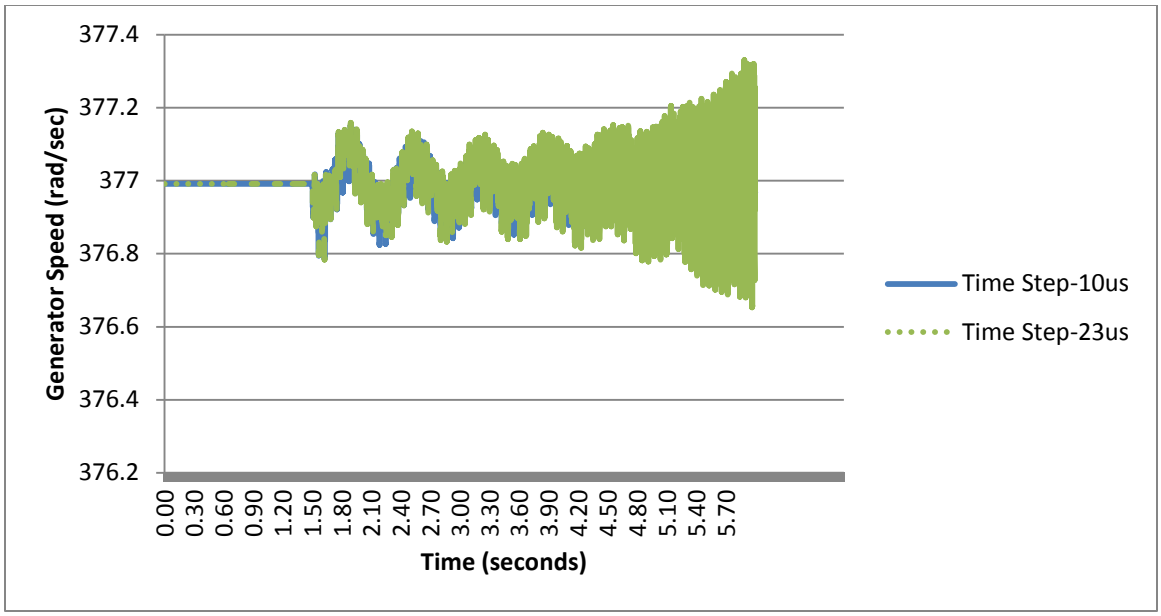

Figure 39 Changes in Generator Speed at Time Steps of 10us and 23us for EMT Model

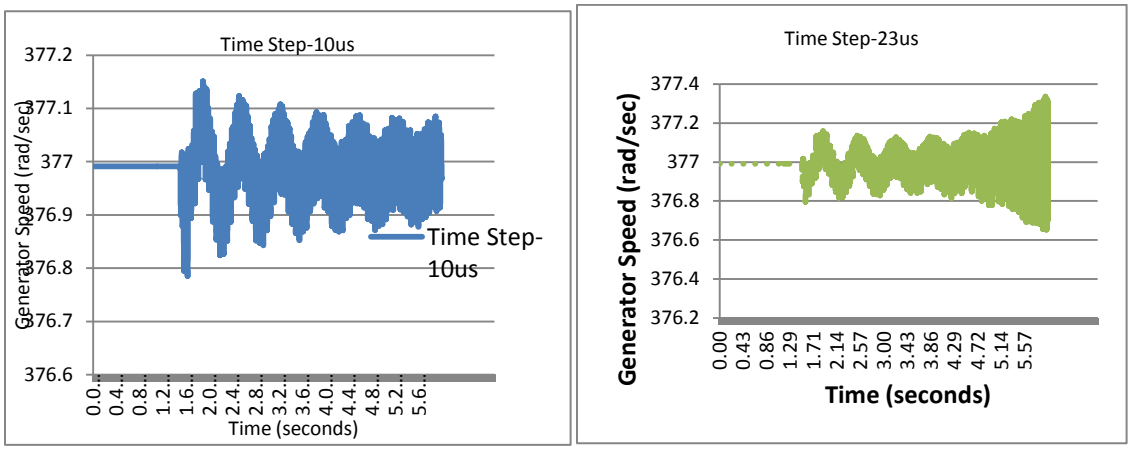

Based on the results shown above, it can be conclude that the DP model using Dynamic Phasor can be simulated with a significantly larger time step as compared to EMT model. It is approximately 30 times larger in the case of sub-synchronous oscillations.

4.6 Conclusions

In this chapter, a Dynamic Phasor model has been developed to analyze oscillations in the sub-synchronous frequency range. This model includes stator dynamics in the generator and LC dynamics in the transmission network. The IEEE first benchmark model for sub-synchronous resonance studies is used as the test system.

Since line compensation is highly dependent upon the level of line compensations for series compensated lines, this model is benchmarked with detailed EMT model at various line compensation levels of the transmission network. The results have shown to give very accurate results, and it can be used to analyze oscillations in this frequency range.

This model also demonstrates the superiority over EMT simulations by increased time steps. The time step used with the proposed model is approximately 30 times larger than the EMT model, thus, it removes the limitation of application to large systems as in EMT environment.

In addition, this model is suitable to analyze sub-synchronous oscillation phenomenon whereas the traditional constant admittance matrix method cannot be utilized.

In conclusion, the oscillations up to 60Hz can be observed with the Dynamic Phasor model.

CHAPTER 5 CONCLUSIONS

5.1 General Conclusion

A transient stability model using Dynamic Phasors has been introduced in this thesis. It is suitable to analyze oscillations up to 60Hz. This model has been compared with detailed EMT simulations, and indicates accurate results in the frequency range of interest. The following summarizes the general process of presenting and validating the DP model in this thesis.

The modeling detail of the generator, Dynamic Phasor representation of the AC network, and the multiple-mass turbine model is presented in Chapter 2 of this thesis. This chapter also briefly introduced the conventional transient stability model as a comparison to the DP model. It presented the background information and foundation for implementing the DP model. The generator model presented is of 8^{th} order, which includes stator dynamics. The stator dynamic is essential in modeling high frequency oscillations in conjunction with the AC network dynamics. The AC network mainly composes of transformers, transmission lines and static loads, and they can be represented using RLC elements. Therefore, it is important to model the LC elements in the network in order to capture the nature of the AC network dynamic behavior. The combining method of the generator and the AC network was also presented in this chapter. This chapter also introduced the modeling detail of a multi-mass turbine system. It was used to validate the DP model for sub-synchronous oscillations.

The DP model was implemented on a SMIB system with parallel transmission lines and the accuracy of the model was validated for low frequency oscillations in Chapter 3. The SMIB system does not contain high frequency oscillations and it is suitable for validating results in the frequency range of less than 3Hz. The model was tested with a 3 phase fault at the middle of one of the transmission lines. The responses of the generator speed and the generator terminal voltage were benchmarked with detailed EMT and the conventional transient stability (PSS/E) results. The simulation results match in all three methods, and shows that the DP method is as accurate as detailed EMT model in analyzing oscillations in the low frequency range.

The accuracy of the DP model in analyzing oscillations in the sub-synchronous frequency range oscillations was validated in Chapter 4. The IEEE first benchmark model was used as the test system. There are minor modifications made to the model in order to ease modeling with Dynamic Phasor, but have no impact on the oscillation responses. The series compensation level of the AC network has direct impact on the electromagnetic oscillation of the system. The value of the series capacitor in the AC network was varied to generate oscillations in the sub-synchronous frequency range. The responses of the generator rotor speed and generator terminal voltage for line compensation levels in the range of 6% to 110% show very close match with detailed EMT simulation results. The results demonstrate that the proposed model is accurate in analyzing sub-synchronous oscillations. The proposed model is also compared to the traditional constant admittance matrix model, and it demonstrated its superiority over the traditional method. As expected, the traditional constant admittance model cannot

observe frequencies above 5Hz, whereas the Dynamic Phasor model can be utilized for frequency range up to 60Hz.

In addition, the DP model allows for use of larger time steps in the integration process as compared to EMT simulations. The integration technique employed is RK4 in this these. The maximum time step can be used without causing any numerical error is 2 times larger than EMT simulations for the SMIB system, and 30 times larger for the IEEE first benchmark model. This demonstrates the possibility of applying this method to large power systems. It eliminates the limitation of small time step requirement in EMT simulations. Due to this requirement, EMT is only suitable for small power systems.

As a final conclusion, the proposed transient stability model is accurate in analyzing oscillations of frequencies up to 60Hz. It also offers the possibility of implementing it in larger power systems as it eliminates the limitation of small time step requirement.

5.2 Contributions

The main contributions of this thesis are listed below.

- Modeled the SMIB system using Dynamic Phasor methodology, and benchmarked results with the detailed EMT equivalent models. The results showed that the DP model can accurately represent low frequency oscillations (<3Hz).

- Modeled the IEEE First Benchmark model using Dynamic Phasor and validated results with equivalent EMT model. Results showed that the DP model can accurately represent oscillations in the sub-synchronous range. This phenomenon cannot be observed with traditional transient stability method, such as in PSS/E and PowerTech software TSAT.
- The time step for integration is shown to be significantly larger than EMT simulations. The integration method used in this thesis is RK4. The time step with the proposed model is shown to be 2 times larger than EMT simulation for the SMIB system, and 30 times larger for the sub-synchronous oscillation model.

5.3 Future works

The main purpose of this thesis is to verify that the Dynamic Phasor model can be used to study oscillations up to the nominal frequency of 60Hz. Following studies can be further performed as a result of this research.

- Use different integration techniques to further increase the time step size, such as trapezoidal and modified RK4,
- Extend the model to a multi-machine system to further verify the validity of the methodology and enhance its application to a large system,
- Develop a hybrid network using the Dynamic Phasor model to model the area of interest and integrate with the rest of the network with traditional transient stability models.

REFERENCES

[1] V Venkarasubramanian, “Tools for dynamic analysis of the general large power system using time-varying Phasors”, Electrical Power and Energy Systems, Vol. 16, no. 6, pp365-376, January 1994.

[2] IEEE/CIGRE Joint Task Force on Stability Terms and Definitions, “Definition and Classification of Power System Stability”, IEEE Transactions on Power Systems, Vol. 19, no. 2, May 2004.

[3] P. Zhang, J. Marti, and H.W. Dommel, “Synchronous Machine Modeling Based on Shifted Frequency Analysis”, IEEE Transactions on Power Systems, Vo. 22, no. 3, August 2007.

[4] A.M. Stankovic, B.C. Lesieutre, and T. Aydin, “Modeling and Analysis of Single-phase Induction Machines with Dynamic Phasors”, IEEE Transactions on Power Systems, Vol. 14, no. 1, February 1999.

[5] C. Karawita, “HVDC Interaction Studies Using Small Signal Stability Assessment”, Ph.D. Thesis, University of Manitoba, April 2009

[6] P. Kundur, “Power System Stability and Control”, McGrew-Hill, Inc, 1994

[7] S. Pekarek, O. Wasynczuk, and H. Hegner, “An Efficient and Accurate Model for the Simulation and Analysis of Synchronous Machine/Converter System”, IEEE Transactions on Energy Conversion, Vol. 13, no. 1, March 1998.

[8]J. J. Grainger, and W. D. Stevenson Jr, “Power System Analysis”, McGrew-Hill, Inc, 1994

[9] M. Parniani, and M.R. Iravani, “Computer Analysis of Small-Signal Stabilit of Power Systems Including Network Dynamics”, IEE Proceedings, Generation, Transmission, Distribution, Vol. 142, no. 6, November 1995

[10] V. Ajjarapu, and C.Christy, “The Continuation Power Flow: A Tool for Steady State Voltage Stability Analysis”, IEEE Transaction on Power Systems, Vol. 7, no. 1, February 1992.

[11] G.S. Vassel, “Northeast Blackout of 1965”, IEEE Power Engineering Review, pp. 4-8, January 1991

[12] T. Demiray, G. Andersson, and L. Busarello, “Evaluation study for the Simulation of Power System Transients using dynamic Phasor Models”, IEEE Transaction, 2008

[13] T. Demiray, and G. Andersson, “Simulation of Power Systems Dynamics using Dynamic Phasor Models”, X Symposium of Specialists in Electric Operational and Expansion Planning, May 2006

[14] Y. Cui, Yan-jun Jian, and Xian-kang Jiang, “Influence of Synchronous Generator Model on Power System Transient Stability”, IEEE 2011

[15] Shao-Ping Huang, Yong-Jian Li, Guo-Bin Jin, and Ling Li, “Simulation Study for Steady-State and Dynamic Performance of the Static Var Compensator”, International Conference on Energy and Environment Technology”, IEEE 2009

[16] Shao-Ping Huang, Guo-Bin Jin, and Ling Li, “Modelling and Simulating for Transient Stability Analysis for Power System using Dynamic Phasor”

[17] S. Kalyani, M. Prakash, and G. Angeline Ezhilarasi, “Transient Stability Studies in SMIB System with Detailed Machine Models”, 2011 International Conference on Recent Advancements in Electrical, Electronics and Control Engineering, 2011

[18] D.H.R. Suriyaarachchi, “Subsynchronous Interactions of a Wind Integrated Power System”, Candidacy Report, University of Manitoba, June 2011

[19] A. Stankovc and T. Aydin, “Analysis of Asymmetrical Faults in Power Systems using Dynamic Phasors”, Power Systems, IEEE Transactions on, Vol. 15, no. 3, pp. 1062-1068, 2000

[20] S. Gomes Jr., N. Martins, A. Stankovic, “Improved Controller Design Using New Dynamic Phasor Models of SVC’s Suitable for High Frequency Analysis”, IEEE, 2006

[21] A.M. Stankovic, H. Lev-Ari, M. M. Perisic, “Analysis and Implementation of Model-Based Linear Estimation of Dynamic Phasors”, IEEE Transactions on Power Systems, Vol. 19, No. 4, November 2004

[22] J.M. Undrill, T.E. Kostyniak, “Subsynchronous Oscillations: Part 1 – Comprehensive System Stability Analysis”, IEEE Transactions on Power apparatus and Systems, Vol. PAS-95, no. 4, July/August 1976

[23] IEEE Subsynchronous Resonance Task Force of the Dynamic System Performance Working Group, Power System Engineering Committee, “First Benchmark Model for Computer Simulation of Subsynchronous Resonance”, IEEE Transactions on Power Apparatus and Systems, Vol. PAS-96, no. 5, September/October 1977

[24] T. Demiray, G. Andersson, “Simulation of Power Systems Dynamics using Dynamic Phasor Models”, X Symposium of Specialists in Electric Operational and Expansion Planning, May 2006

[25] M.A. Hannan, K. W. Chan, “Transient Analysis of Facts and Custom Power Devices using Phasor Dynamics”, Journal of Applied Sciences 6(5): 1074-1081, 2006

[26] P. Mattavelli, G.C. Verghese, A. M. Stankovic, “Phasor Dynamics of Thyristor-Controlled Series Capacitor Systems”, IEEE Transactions on Power Systems, Vol. 12, No. 3, August 1997

[27] P.M. Anderson, B.L. Agrawal, J.E. Van Ness, “Subsynchronous Resonance in Power Systems”, IEEE Press, The Institute of Electrical and Electronics Engineers, Inc., New York, 1989

APPENDIX A

Single Machine Infinite Bus Test System

A.1 Test System Configuration

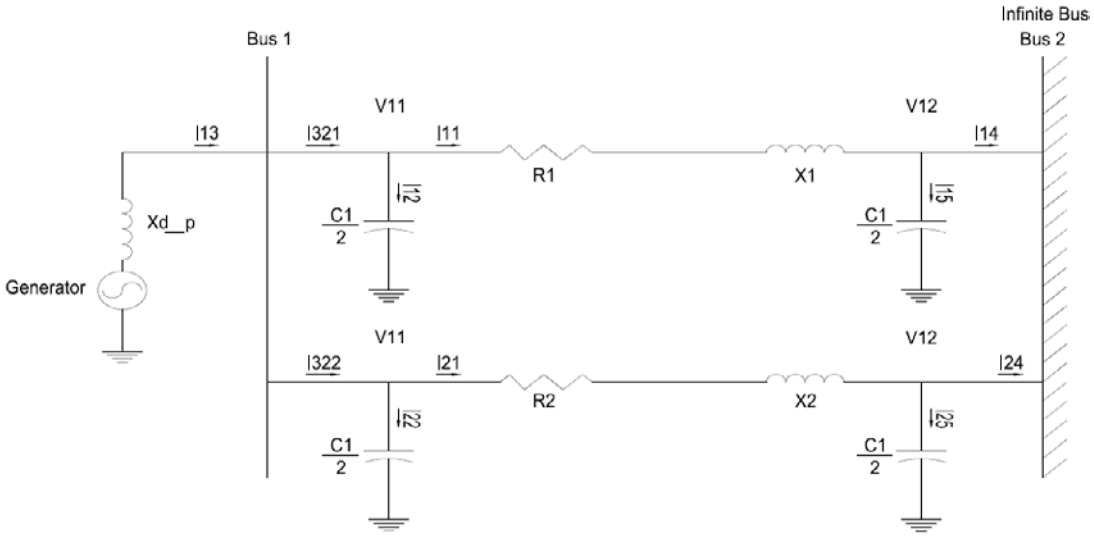

Figure A.1 Single Machine Infinite Bus System

A.2 Test System Data

A.2.1 Power Flow – AC Bus Data

Bus	Voltage	
Number	Magnitude (pu)	Angle (radians)
1	1.1909	0.1942
2	1	0

A.2.2 Power Flow – Generator Data

Bus Number	MW	Mvar
1	477.7366	335.6908
2	450	217.9449

A.2.3 Power Flow – Line Data

		Series		Charging	
From Bus Number	To Bus Number	Resistance (pu)	Reactance (pu)	Conductance (pu)	Susceptance (pu)
1	2	0.125	0.625	0.0000	0.0078
1	2	0.125	0.625	0.0000	0.0078

A.2.4 Dynamic – Generator Data

IBUS	MVA	T'do (pu)	T"do (pu)	T'qo (pu)	T"qo (pu)	H (pu)	D (pu)	Xd (pu)	Xq (pu)	X'd (pu)	X'q (pu)	X"d (pu)	Xl (pu)
1	555	8.0683	0.03	1.0007	0.07	3.5	0.0	1.935	1.885	0.425	0.775	0.355	0.275

A.2.5 AC Network Dynamic Phasor Equations

$$\frac{d}{dt}(I11\_re) = \frac{Wo}{L1}(V1_{re} - V2_{re} - R1I11_{re}) + w0(I11_{im}) \quad \text{(A.1)}$$

$$\frac{d}{dt}(I11\_im) = \frac{Wo}{L1}(V1_{im} - V2_{im} - R1I11_{im}) - w0(I11_{re}) \quad \text{(A.2)}$$

$$\frac{d}{dt}(I21\_re) = \frac{Wo}{L2}(V1_{re} - V2_{re} - (R2)I21_{re}) + w0(I21_{im}) \quad \text{(A.3)}$$

$$\frac{d}{dt}(I21\_im) = \frac{Wo}{L2}(V1_{im} - V2_{im} - (R2)I21_{im}) - w0(I21_{re}) \quad \text{(A.4)}$$

$$\frac{d}{dt}(V1_{re}) = \left(\frac{1}{c}\right)(I13_{re} - I11_{re} - I21_{re}) + w0V1_{im} \quad \text{(A.5)}$$

$$\frac{d}{dt}(V1_{im}) = \left(\frac{1}{c}\right)(I13_{im} - I11_{im} - I21_{im}) - w0V1_{re} \quad \text{(A.6)}$$

APPENDIX B

IEEE First Benchmark Model

B.1 IEEE First Benchmark Model Test System

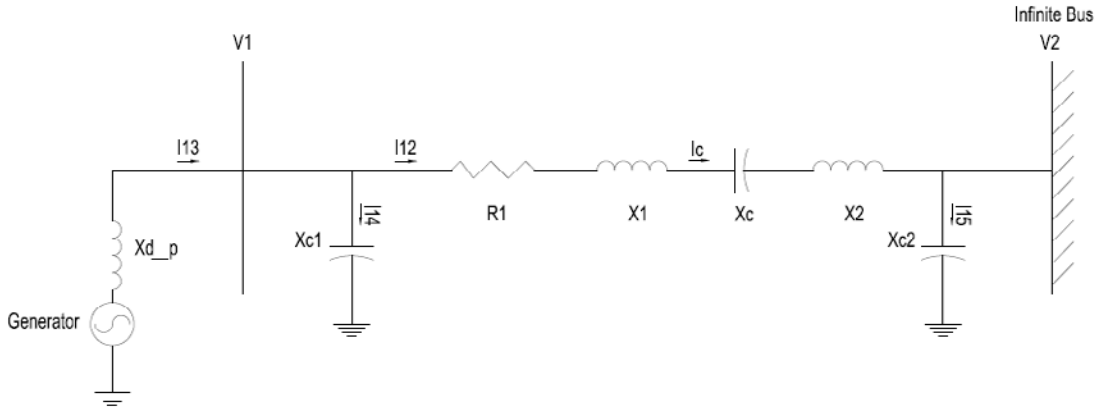

Figure B.1.1 IEEE First Benchmark Model for Sub-synchronous Resonance Test System

B.2 Test System Data

B.2.1 Power Flow – AC Bus Data

Bus	Voltage	
Number	Magnitude (pu)	Angle (radians)
1	1.1	-0.4
2	1	-0.0665

B.2.2 Power Flow – Generator Data

Bus Number	MW	Mvar
1	803.16	388.9881

B.2.3 Power Flow – Line Data

		Series			Charging
From Bus Number	To Bus Number	Resistance (ohm)	Inductance (H)	Capacitance (μF)	Capacitance (μF)
1	2	6.832	0.4323	21.66	5.5

B.2.4 Dynamic – Generator Data

IBUS	MVA	T'do (pu)	T"do (pu)	T'qo (pu)	T"qo (pu)	H (sec)	D (pu)	Xd (pu)	Xq (pu)	X'd (pu)	X'q (pu)	X"d (pu)	X"q (pu)	Xl (pu)
1		4.3	0.032	0.85	0.05	0.868495	0	1.79	1.71	0.169	0.228	0.135	0.2	0.131

B.2.5 Dynamic – Multi-Turbine Data

Mass	Inertia H (seconds)	Torque (pu)	Shaft	Spring Constant (pu Torque/rad)
HP	0.092897	0.3*Te	HP-IP	19.303
IP	0.155589	0.26*Te	IP-LPA	34.929
LPA	0.858670	0.22*Te	LPA-LPB	52.038
LPB	0.884215	0.22*Te	LPB-GEN	7.0858
GEN	0.868495	Te	n/a	n/a

APPENDIX C

List of Principal Symbols

J	Moment of inertia of the rotr mass
t	time
P_m	Mechanical power
P_e	Electrical power
T_m	Mechanical torque
T_e	Electrical torque
θ	Angular position of the rotor
H	Inertia constant
S_{rated}	Generator MVA rating
f_d	Field winding
k_d	d-axis amortisseur circuit
k_q	q-axis amortisseur circuit
ω	Angular frequency